

Geologica Acta: an international earth science journal

ISSN: 1695-6133

geologica-acta@ija.csic.es

Universitat de Barcelona

España

ARENILLAS, I.; ARZ, J.A.; GRAJALES-NISHIMURA, J.M.; MELÉNDEZ, A.; ROJAS-CONSUEGRA, R.

The Chicxulub impact is synchronous with the planktonic foraminifera mass extinction at the Cretaceous/Paleogene boundary: new evidence from the Moncada section, Cuba Geologica Acta: an international earth science journal, vol. 14, núm. 1, marzo, 2016, pp. 35-51

Universitat de Barcelona Barcelona, España

Available in: http://www.redalyc.org/articulo.oa?id=50544801004



Complete issue

More information about this article

Journal's homepage in redalyc.org



The Chicxulub impact is synchronous with the planktonic foraminifera mass extinction at the Cretaceous/Paleogene boundary: new evidence from the Moncada section, Cuba

I. ARENILLAS¹ J.A. ARZ¹ J.M. GRAJALES-NISHIMURA² A. MELÉNDEZ¹ R. ROJAS-CONSUEGRA³

Departamento de Ciencias de la Tierra e Instituto de Investigación en Ciencias Ambientales (IUCA), Universidad de Zaragoza

Pedro Cerbuna 12, 50009 Zaragoza, Spain. Arenillas E-mail: ias@unizar.es Arz E-mail: josearz@unizar.es Meléndez E-mail: amelende@unizar.es

²Instituto de Geología, Universidad Nacional Autónoma de México

Ciudad Universitaria, Coyoacán, México D.F., 04510, México. E-mail: mgrajales@geologia.unam.mx

³Museo Nacional de Historia Natural

Obispo 61, Plaza de Armas Habana Vieja, 10100 La Habana, Cuba. E-mail: rojas@mnhnc.inf.cu

\dashv ABSTRACT \vdash

The Moncada section, western Cuba, is one of the few sections across the Cretaceous/Paleogene (K/Pg) boundary in the Gulf of Mexico and Caribbean where an Ir anomaly has been identified toward and above the top of a clastic unit, locally called the Moncada Formation (Fm.). The Moncada Fm. is enriched in ejecta (altered glass spherules, shocked quartz, melt rock fragments, etc.) and represents the local Complex Clastic Unit (CCU) linked to the Chicxulub impact event. This CCU is overlain by a 2-3cm thick bed of Ir-rich, dark, calcareous claystone which represents the "K/T Boundary Clay" at Moncada. All lowermost Danian Planktonic Foraminiferal zones and Acme-Stages (PFAS) were identified, suggesting stratigraphic continuity across the Danian and indicating that the Moncada Fm. is K/Pg boundary in age. High-resolution biostratigraphic data suggest that the mass extinction event of planktonic foraminifera at the K/Pg boundary was more severe than previously suggested. The absence of cosmopolitan, generalist Cretaceous species in the Danian deposits of Moncada supports the hypothesis that only Guembelitria survived the mass extinction triggered by the Chicxulub impact event. The high Ir-concentration and the ejecta-rich clay laminations identified in the lowermost Danian of Moncada (Ancón Fm.) are explained partly as the redeposition of ejecta material eroded and reworked from higher topographic levels, still contaminated by toxic trace elements (e.g., Cu and Ni) of meteoritic origin. These pollutants of meteoritic origin could have affected the ecological conditions of the pelagic environment for thousands of years after the K/Pg boundary, being particularly intense just after the Chicxulub impact. The ecological stress due to the pollutants partly explains the catastrophic mass extinction of planktonic foraminifera at the K/Pg boundary and their subsequent evolutionary radiation.

KEYWORDS

CCU. Ejecta. "K/T Boundary Clay". Danian. PFAS.

INTRODUCTION

One of the most passionate debates in the Earth sciences focuses on the end-Cretaceous mass extinction and its

relation with the eruption of the massive Deccan volcanic province, India (Chenet *et al.*, 2007; Schoene *et al.*, 2015), and/or with the Chicxulub asteroid impact on Yucatan, Mexico, 66Ma ago (Hildebrand *et al.*, 1991; Schulte *et al.*,

2010). The huge disturbance triggered by the Chicxulub impact in the continental margins caused the deposition of distinctive eventites of ejecta-rich clastic material around the Gulf of Mexico and the Central American region (Smit et al., 1992; Bohor, 1996; Takayama et al., 2000; Arz et al., 2001; Grajales-Nishimura et al., 2009; Denne et al., 2013). These eventites have been collectively called the "K/T boundary cocktail" by Bralower et al. (1998) or the Complex Clastic Unit (CCU) by Arenillas et al. (2006). Sedimentological analyses suggest that CCUs are finingupward sedimentary successions that represent a single graded, high-density flow deposit probably accumulated in hours, days or weeks, and partially reworked by megatsunami currents (Maurrase and Sen, 1991; Bralower et al., 1998; Soria et al., 2001; Goto et al, 2008). Other authors have proposed that CCUs and the Chicxulub impact are not related to the K/Pg boundary mass extinction event, suggesting that the former predated the K/Pg boundary by ~300kyr (Keller *et al.*, 2003, 2007).

Although their thickness, lithology and sedimentology are different in each locality depending on their proximity to the impact site, the source area of clastic material, and the sedimentary depositional environment, all the CCUs have in common the presence of ejecta (i.e., spherules, shocked minerals, Ni-rich spinels, highly-concentrated Ir, etc.) derived from the Chicxulub impact site (Smit, 1999; Claeys et al., 2002). In localities near to Chicxulub (e.g., SE Mexico, Cuba) the CCU is usually an eventite of decameter to hectometer thickness, beginning with a thick carbonate or polymictic breccia, and ending with fine-grained ejecta-spherule-rich sandstones, capped by a thin, Ir-rich silty layer (Montanari et al., 1994; Grajales-Nishimura et al., 2000, 2009; Takayama et al., 2000; Tada et al., 2002, 2003; Alegret et al., 2005; Goto et al., 2008). In more distant and/or deeper localities (e.g., Haiti, NE Mexico) the CCU is around a meter in thickness, with a basal bed of coarse spherules, followed by fine-grained sandstones, and in some localities also terminates with a thin Ir-rich clay layer (Maurrasse and Sen, 1991; Smit, 1999; Arz et al., 2001; Maurrasse et al., 2005). In localities that are even more distant and/or deeper (e.g., Black Nose and Bass River in the NW Atlantic, Ocean Drilling Program (ODP) Sites 999B and 1001B in the Caribbean Sea, and Demerara Rise in the SW Atlantic), the eventite is already very different from the typical CCU, consisting only of a centimeter- to decimeter-thick bed with spherules and an Ir anomaly in its upper part (Olsson et al., 1997; Norris et al., 1999; Martínez-Ruiz et al., 2001; Huber et al., 2002; MacLeod et al., 2007).

The identification of continuous stratigraphical sections across the Cretaceous and Paleogene around the site of the meteorite impact, at least in the basal Danian, as well as the micropaleontological study of them with a high-resolution

methodology, is indispensable for accurately analyzing the age of the Chicxulub-linked CCU. In order to accomplish this objective, the most continuous K/Pg sections closest to the Chicxulub crater must be intensively studied. The interest of the Moncada section, western Cuba, lies in it being one of the few K/Pg boundary sections in Cuba where an Ir anomaly (over 800ppt) has been identified (Tada et al., 2002). The main aims of this paper are to perform a high-resolution quantitative biostratigraphic study of the section with planktonic foraminifera and a petrographic analysis of shocked minerals, and to provide new evidence that corroborates the relationship of the Chicxulub impact with the K/Pg boundary mass extinction. Additionally, we focus on an analysis of the paleoenvironmental effects in the earliest Danian planktonic foraminiferal assemblages, and describe the sequence of events and episodes in pelagic environments after the K/Pg boundary.

GEOLOGICAL SETTING

The Moncada section, first identified by Iturralde-Vinent (1995), is located near to the village of Moncada (22°36'N, 83°45'W), in the Sierra de Los Órganos, 18km west of Viñales and 4km east of Pons, in Pinar del Río Province, western Cuba (Fig. 1A). This section is placed in Los Órganos belt, which, together with the adjacent Rosario belt (in the Sierra del Rosario), is part of the Guaniguanico terrane in western Cuba (Fig. 1A; Pszczólkowski, 1987; García and Torres, 1997). The allochthonous nature of the Guaniguanico terrane has been discussed in the Cuban literature (Iturralde-Vinent, 1998, 2012; Bralower and Iturralde-Vinent, 1997), and its original location is estimated to have been in the western margin of the Yucatan platform, ~400km east of the Chicxulub crater (Fig. 1B). According to these authors, the Moncada materials were deposited at upper bathyal depths, and were moved to their present location by tectonic forces. The CCU, locally named the Moncada Fm., is characterized by a 2m thick deposit, which consists of calcareous sandstones in its lower-middle part and an alternation of calcareous clays and very-fine sandstone in its upper part (Fig. 2). This formation disconformably overlies 2m of grayish-black, bedded micritic limestone of the Pons Fm. (Albian), with a slightly undulating erosional surface, and is conformably overlain by 1.25m of marly limestone of the Ancón Fm. (Danian), with a gradational contact (Fig. 2).

The Moncada Fm. was initially related to the Chicxulub impact by Iturralde-Vinent (1995). Later, Tada *et al.* (2002) described this stratigraphic interval in detail as a calcareous sandstone complex composed of five sandstone units (U1 to U5), reproduced here in Figures 2 and 3. According to Tada *et al.* (2002), these units decrease upward in thickness and maximum grain size, and their boundaries are no

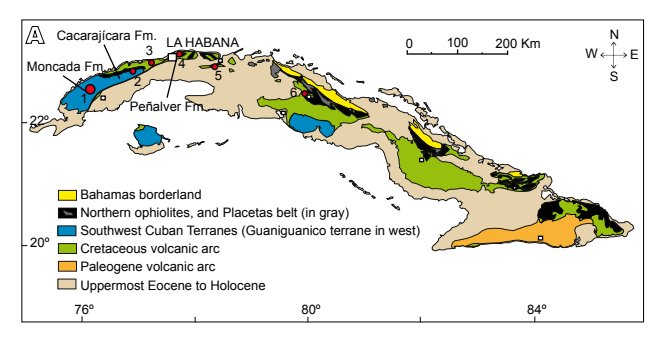




FIGURE 1. A) Geologic structure and subdivision of tectonic units in Cuba, and location of the most significant K/Pg sections and related formations. 1: Moncada, 2: Cacarajícara, 3: Santa Isabel, 4: Peñalver, 5: Cidra, and 6: Loma Capiro; B) Paleogeographic reconstruction of Gulf of Mexico and the Caribbean region during the K/Pg transition (modified from Blakey, 2011), and locations of some of the main K/Pg sections in these regions, foregrounding the Cuban sections with larger letters.

erosional contacts. Each unit shows upward fining and changes in sedimentary structures, from thin parallel beds to parallel laminations, and then to flaser and/or lenticular bedding with ripple cross-laminations. This suggests deposition from flowing currents with a gradual decrease in flow speed in the units. The paleocurrent directions are unidirectional in individual units, but exhibit patterns of current reversals suggesting a tsunami origin.

This sequence is overlain by a 2-3cm thick unit of alternating dark-colored, calcareous claystones and very fine calcareous sandstones, and ends with a 1-2cm thick, olive-gray, fine sandstone layer with a yellowish rim (Fig. 3). Tada *et al.* (2002) named this thin stratigraphic interval at the top of the Moncada Fm. as UpperMost Unit (UMU), and it is relevant to the stratigraphy of the K/Pg boundary because it contains a dark clay bed (UMU-1) enriched in Ir (between 380 and 450ppt). The upper boundary of the UMU is bioturbated, and the upper 1cm thick sandstone (UMU-2) grades upward into the marly limestone of the Ancón Fm. UMU-2 has an Ir concentration between 160 and 220ppt. The first 3 centimeters of the Ancón Fm. are

also bioturbated, and strongly enriched in Ir. The Ancón Fm. includes micritic and marly limestones, with frequent parallel lamination. According to Tada *et al.* (2002), the Ir concentration reaches a maximum of 815ppt in the 1cm thick yellowish marly limestone of the basal part of the Ancón Fm., and gradually descends until reaching a value of 13ppt 40cm above this (Fig. 3).

MATERIAL AND METHODS

For micropaleontological analysis, 26 samples across the critical K/Pg boundary interval were collected in the Moncada section (Fig. 2). In the Pons Fm. and CCU samples, there were too few planktonic foraminifera for quantitative studies probably due to taphonomic and diagenetic factors. In the Ancón Fm., planktonic foraminifera are relatively more abundant, but specimens are recrystallized, partially dissolved and deformed, and most of the specimens are internal moulds. Although these taphonomic factors must be taken into account, the planktonic foraminifera are still well enough preserved to permit rigorous taxonomic identification and consistent biostratigraphic studies.

Because all the samples were very lithified, they were processed using a disaggregating technique, employing a solution with 80% acetic acid and 20% H₂O. Samples were dried at ≤50°C, and sieved into 38-63µm and ≥63µm size fractions. All specimens were identified, sorted, and fixed on standard 60-square micropaleontological slides. The best-preserved specimens were examined under the scanning electron microscopes (SEM) JEOL JSM 6400 and Zeiss MERLIN FE-SEM at the Electron Microscopy Service of the Universidad de Zaragoza (Spain). Lower Danian planktonic foraminiferal species of biochronostratigraphic importance are illustrated in Figure 4.

The 125cm thick Ancón Fm. was sampled (19 samples) at high-resolution, i.e., at intervals of centimeters in the lower part to decimeters in the upper part. For the quantitative analyses (Table 1), a split of about 250 planktonic foraminiferal specimens from the ≥63µm size fraction was picked from the lower Danian of Moncada using an Otto splitter. Here, we used the lower Danian planktonic foraminiferal zonations of Arenillas et al. (2004). The Hedbergella holmdelensis subzone of Arenillas et al. (2004) is the most relevant for this study because it is the first Danian subzone, and it is defined as the stratigraphic interval between the highest occurrence of Plummerita hantkeninoides (or K/Pg mass extinction of planktonic foraminifera) and the lowest occurrence of Parvularugoglobigerina longiapertura. The Figure 2 shows the equivalence between this biozonation and that of Berggren and Pearson (2005), which is the most widely used. Because Berggren and Pearson (2005)

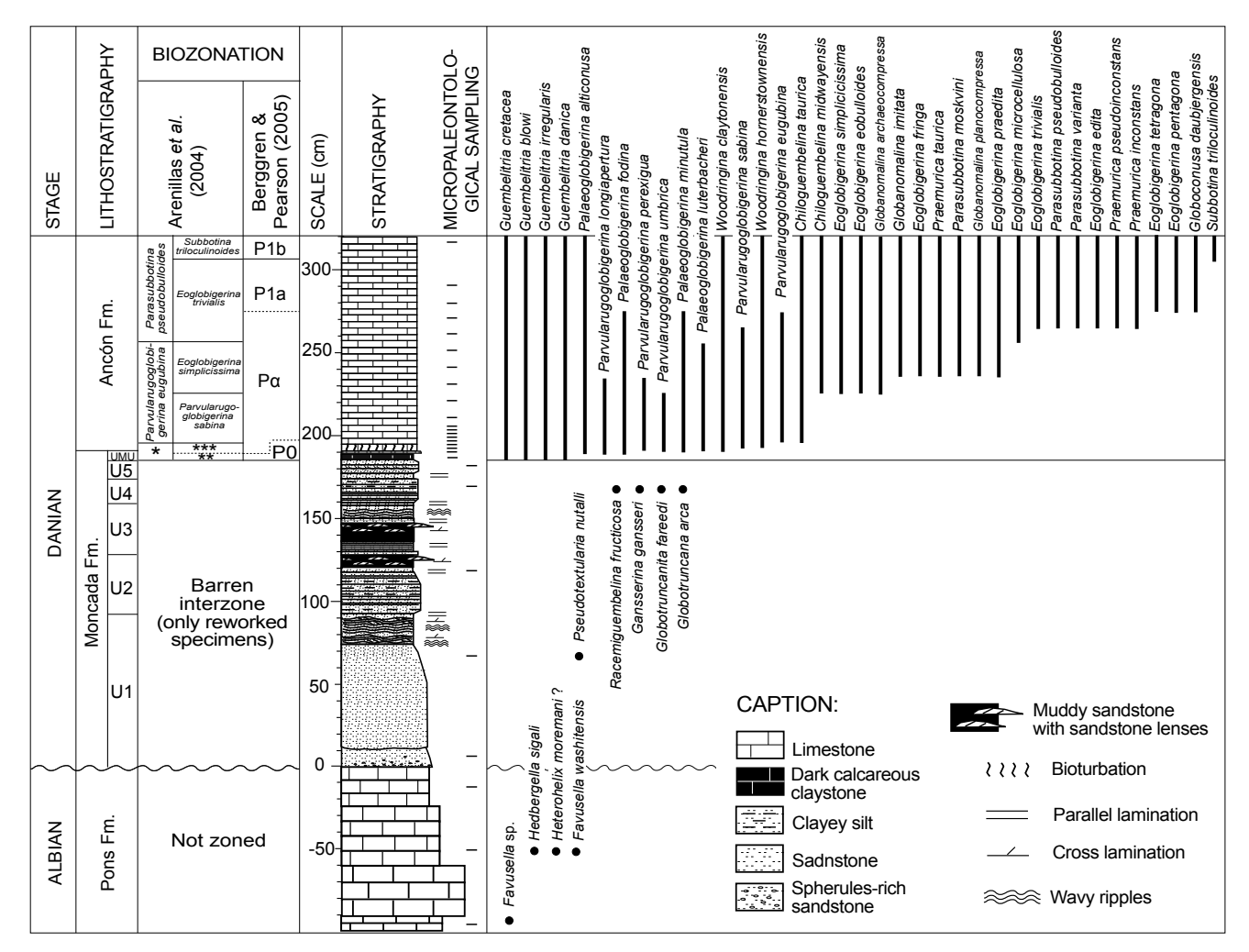


FIGURE 2. Lithostratigraphic formations and units of Tada *et al.* (2002), planktonic foraminiferal zonations, micropaleontologial sampling, and stratigraphic distribution of planktonic foraminiferal species. *Guembelitria cretacea zone, **Hedbergella holmdelensis subzone, ***Parvularugoglobigerina longiapertura subzone.

considered *Pv. longiapertura* to be a junior synonym of *Parvularugoglobigerina eugubina*, the *Hedbergella holmdelensis* subzone is considered equivalent to their zone P0 (Fig. 2). According to Arenillas *et al.* (2004), the calibrated numerical ages of the biozonal boundaries approximately indicate that the *Hedbergella holmdelensis* subzone spans the first 6kyr after the K/Pg boundary, the *Parvularugoglobigerina longiapertura* subzone from 6 to 20kyr, the *Parvularugoglobigerina simplicissima* subzone from 37 to 60kyr, the *Eoglobigerina simplicissima* subzone from 60 to 280kyr, and the *Subbotina triloculinoides* subzone from 280kyr on.

High-resolution quantitative biostratigraphic studies in Tethyan sections enable to recognize three Planktonic Foraminiferal Acme Stages (PFAS) across the lowermost Danian in oceanic- and outer neritic-pelagic environments (see Arenillas *et al.*, 2006): PFAS-1, dominated by triserial *Guembelitria*, spans approximately

the first 10kyr after the K/Pg boundary; PFAS-2, dominated by tiny trochospiral parvularugoglobigerinids (*Parvularugoglobigerina* and *Palaeoglobigerina*), spans approximately from 10 to 50kyr; and PFAS-3, dominated by biserial *Woodringina* and *Chiloguembelina*, spans from 50kyr on. Because the taxonomic identification of some species is difficult in samples from the Moncada section due to the poor preservation, the documentation of the PFAS stages is particularly useful for checking the stratigraphic continuity between the Moncada and Ancón formations, because they do not involve problematic taxonomic assignments.

In order to characterize the groundmass of samples from the ejecta layer and the types, size and shapes of rock, altered glass and mineral fragments, we applied standard macroscopic and light microscope methods. A Carl Zeiss standard polarizing petrographic microscope with an integrated AmScope digital camera was used to perform the petrographic analysis of eight polished thin sections,

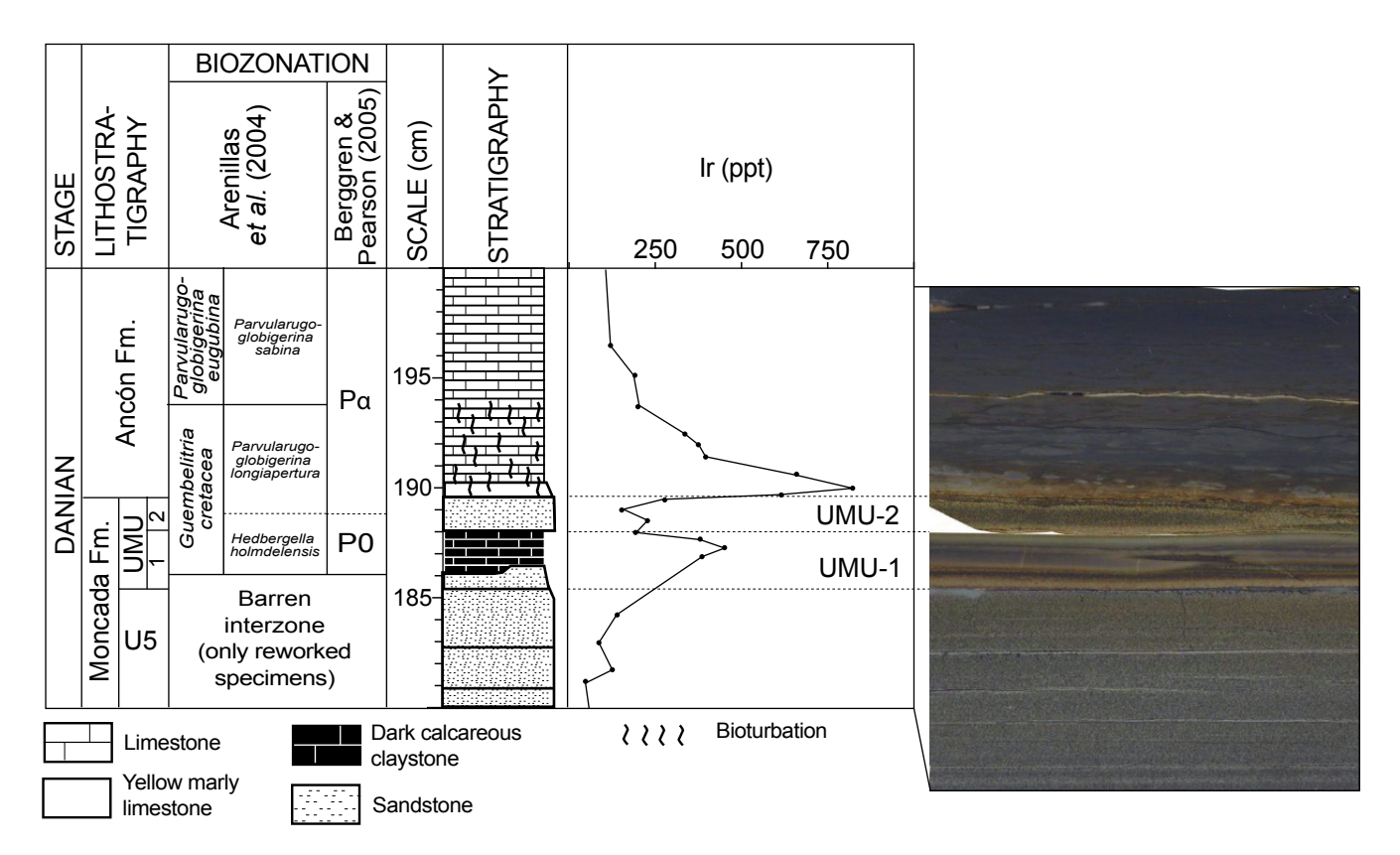


FIGURE 3. Detail of the Ir concentration profile and polished-section of the uppermost CCU (subunit U5), K/Pg boundary clay bed (UMU) and lowermost Ancón Fm. (according to Tada et al., 2002).

four from the Moncada Fm., two from the UMU and two from the basal part of the Ancón Fm.

EVIDENCE OF SYNCHRONICITY

In the Gulf of Mexico and the Caribbean region, the presence of shocked minerals, accretionary lapilli and millimeter-sized spherules compositionally linked to the Chicxulub impact site, some with a preserved glass core, is common in the CCU deposits (Izett et al., 1990; Sigurdsson et al., 1991; Maurrasse and Sen, 1991; Grajales-Nishimura et al., 2009). If the uppermost subunit of the CCU is present, a high Ir concentration toward the top of the CCU, usually composed of fine sand, silt and/or clay, is also common (Smit, 1999). In the absence of radiometric data, to check the synchronicity of the deposition of the CCU with the Chicxulub impact and the K/Pg boundary mass extinction event, mineralogical and micropaleontological evidence is necessary.

Mineralogical and petrographic evidence

The Moncada Fm. is represented by a fining-upward sedimentary silicate and calcareous clastic sedimentary sequence, composed of mixtures of different concentrations of lithoclasts and ejecta particles. Previous petrographic observations had revealed the occurrence of abundant shocked quartz grains and whitish vesicular fragments throughout the Moncada Fm. Vesicular fragments preserve the quench texture of clinopyroxene, suggesting their impact melt origin (Tada *et al.*, 2003). Under the optical microscope, the groundmass between the melt fragments is heterogeneous. In Figure 5, various petrographic features are shown at several scales and described at length in captions.

The basal part of the Moncada Fm. (lower part of U1 of Tada *et al.*, 2002) is constituted by ejecta material composed of fine gravel to coarse sand-sized particles. Its composition is mainly represented by melt rock fragments and smectite spherules, surrounded by a matrix of smectite fragments, as well as quartz grains and clay minerals. Clinopyroxene quench texture is common in some smectite-altered vesicular fragments (Fig. 5A, B). Some of the melt grains are 5.5mm in diameter and are composed of smectite-altered glass and inclusions of quartz schist (Fig. 5C). Altered smectite or calcite spherules are 1, 2 and up to 3mm in diameter.

The lower part of the Moncada Fm. (upper part of U1) corresponds to sand-sized ejecta material and is composed

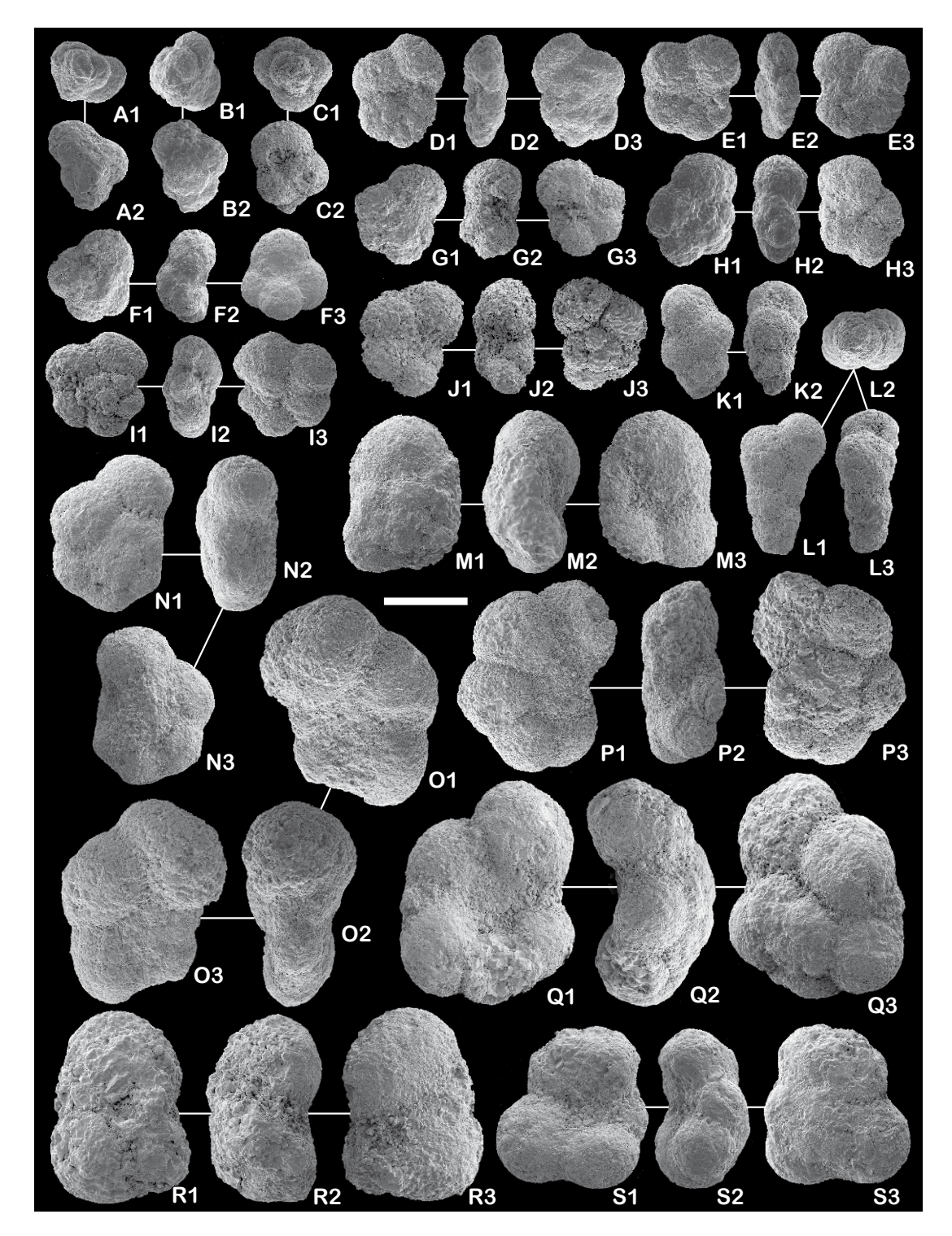


FIGURE 4. Lower Danian planktonic foraminiferal species identified in the UpperMost Unit of the Moncada Fm. (UMU) and the Ancón Fm. (Scale bar = 100µm). A-B) Guembelitria cretacea Cushman, 1933, from the H. holmdelensis subzone in UMU-1 (A) and Pv. sabina subzone (B). C) Guembelitria blowi (Arz, Arenillas and Náñez, 2007), from the E. simplicissima subzone. D-E) Parvularugoglobigerina longiapertura (BLow, 1979), from the Pv. sabina subzone (D). and Pv. longiapertura subzone (E). F) Palaeoglobigerina fodina (BLow, 1979), from the Pv. sabina subzone. G-H) Parvularugoglobigerina sabina (Luterbacher and Premoli Silva, 1964), from the Pv. sabina subzone. I-J) Parvularugoglobigerina eugubina (Luterbacher and Premoli Silva, 1964), from the Pv. sabina subzone. K) Woodringina hornerstownensis Olsson, 1960, from the Pv. Sabina subzone. M) Eoglobigerina simplicissima (BLow, 1979), from the S. triloculinoides subzone. N) Globanomalina archeocompressa (BLow, 1979), from the E. trivialis subzone. Q) Praemurica taurica (MOROZOVA, 1961), from the E. trivialis subzone. Q) Praemurica inconstans (Subbotina, 1953), from the E. trivialis subzone. R) Subbotina triloculinoides (PLUMMER, 1928), from the S. triloculinoides subzone. S) Eoglobigerina trivialis (Subbotina, 1953), sensu Blow (1979), from the S. triloculinoides subzone.

TABLE 1. Relative abundance of planktonic foraminifera species and genera of the lowermost Danian at Moncada

18	18.9 12.9 11.8 18.3 24.2 14.7 12.5 7.1 9.3 1.8 1.8 10.2 13.1 11.1 12.0 8.5 5.5 64 0.9 3.5 2.7 8.6 7.7 6.7 4.0 6.7 6.4 7.2 11.1 8.0 4.0 6.7 6.7 6.4 9.4 6.7 6.4 8.8 7.0 11.1 3.4 6.9 4.0 6.7 6.4 7.3 8.4 13.7 8.8 7.0 17.1 5.8 6.7 9.3 9.7 12.7 8.8 7.0 17.1 5.8 6.7 9.3 9.7 12.7 1.8 8.0 4.6 11.1 11.1 13.3 10.5 6.4 1.1 1.1 1.1 11.1 13.3 10.5 6.4 1.1 1.1 1.1 11.1 13.3 10.5 6.4 1.1 1.1 1.1 11.1 13.3 10.5 6.4 1.1 1.1 1.1 1.1 13.3 1.2 1.2 1.1 1.2 1.3 1.3 1.7 1.4 1.4		0.8.0.4.4.0.8.0.0.0.0.0.0.0.0.0.0.0.0.0.	2.2. 0.0 0.0 0.0 0.0 0.0 0.0 0.0 0.0 0.0	1.8 0.5 0.5 0.5 0.0 0.3 0.3 0.3 0.3 0.3 0.3 0.3 0.3 0.3
Herea 18 102 13.1 11.1 12.0 8.5 5.5 6.4 4.5 6.9 12.7 17.1 12.0 8.5 5.5 6.4 4.5 6.9 12.2 17.1 17.3 10.5 6.4 13.7 12.3 12.3 12.3 12.3 12.3 12.3 12.3 12.3	1.8 1.8 1.0 13.1 11.1 12.0 8.5 5.5 64 0.9 1.2 2.7 1.7 10 8.9 4.0 6.7 4.0 4.6 3.4 0.9 3.5 2.7 8.6 7.7 6.7 4.0 6.7 6.4 7.2 11.1 8.0 4.0 4.0 6.7 4.0 6.4 8.8 7.0 17.1 5.8 6.7 9.3 9.7 12.7 1.8 8.0 4.6 11.1 11.1 13.3 10.5 6.4 1.8 8.0 4.6 11.1 11.1 13.3 10.5 6.4 1.8 8.0 4.6 11.1 11.1 13.3 10.5 6.4 1.8 8.0 4.6 11.1 11.1 13.3 10.5 6.4 1.8 8.0 4.6 11.1 11.1 11.1 13.3 10.5 6.4 1.1 1.1 11.1 11.1 11.1 11.1 11.2 8.2 8.2 1.8 8.0 4.0 4.0 11.2 11.2 8.4 6.4 1.8 5.9 4.0 2.9 <t< td=""><td>8. 8. 4. 4. 4. 4. 4. 4. 4. 4. 4. 4. 4. 4. 4.</td><td></td><td></td><td></td></t<>	8. 8. 4. 4. 4. 4. 4. 4. 4. 4. 4. 4. 4. 4. 4.			
Sea	0.9 1.2 2.7 1.7 1.0 2.0 4.0 4.6 3.4 0.9 3.5 2.7 8.6 7.7 6.7 4.0 4.6 3.4 0.9 3.5 2.7 8.6 7.7 6.7 4.0 4.7 3.8 8.4 13.7 8.8 7.0 17.1 5.8 6.7 9.3 9.7 12.7 12. 11.1 8.0 4.0 4.6 13.2 8.8 7.0 17.1 5.8 6.7 9.3 9.7 12.7 12.7 13.1 13.3 10.5 6.4 13.7 13.8 13.2 13.2 13.2 13.2 13.2 13.2 13.2 13.2	2			
Sea	1.7 1.7 1.0 6.7 6.4 0.9 3.5 2.7 8.6 7.7 6.7 4.0 4.6 3.4 0.9 3.5 2.7 8.6 7.7 6.7 4.0 4.6 3.4 0.4 0.9 3.5 2.7 8.6 7.7 6.7 4.0 4.6 3.4 13.7 0.9 9.6 14.3 16.9 9.8 7.3 10.9 13.2 8.8 7.0 17.1 5.8 6.7 9.3 9.7 12.7 12.7 12.8 12.9 9.8 7.0 17.1 5.8 6.7 9.3 9.7 12.7 12.7 12.8 12.9 13.2 12.9 13.2 12.9 13.2 12.9 13.2 12.9 13.2 12.9 13.2 12.9 13.2 12.9 13.2 12.9 13.2 12.9 13.2 12.9 13.2 12.9 13.2 12.9 13.2 13.2 13.2 13.2 13.2 13.2 13.2 13.2	2. 4. 4. 8. 8. 4. 4. 8. 8. 4. 7. 5. 5. 6. 8. 8. 4. 7. 5. 6. 8. 8. 4. 7. 5. 6. 8. 8. 4. 7. 5. 6. 8. 8. 4. 7. 5. 6. 8. 8. 4. 7. 5. 6. 8. 8. 4. 7. 5. 6. 8. 8. 4. 7. 5. 6. 8. 8. 4. 7. 5. 6. 8. 8. 4. 7. 5. 6. 8. 8. 7. 7. 7. 7. 8. 8. 7. 7. 7. 7. 8. 8. 7. 7. 7. 7. 8. 8. 7. 7. 7. 7. 8. 8. 7. 7. 7. 7. 8. 8. 7. 7. 7. 7. 7. 8. 8. 7. 7. 7. 7. 7. 7. 7. 7. 7. 7. 7. 7. 7.			
Sea	1.1 34 8.9 4.0 6.7 6.4 8.9 4.0 6.7 6.4 8.9 8.9 4.0 6.7 6.4 8.9 8.9 8.7 6.7 4.0 4.6 3.4 9.9 8.9 7.0 17.1 5.8 6.7 9.3 9.7 12.7 1.8 8.0 4.0 17.1 5.8 6.7 9.3 9.7 12.7 1.8 8.0 4.6 11.1 11.1 13.3 10.5 6.4 12.7 12.7 12.7 12.8 12.9 12.2 12.2 12.3 12.3 12.3 12.3 12.3 12.3	8.4.1.6.6.7.7.8.8.4.1. 8.4.1.6.0.7.7.8.8.4.1. 7. 8.4.1.2. 7. 8.4.1.			
Scale	72 11.1 80 4.0 4.3 4.4 7.3 8.4 13.7 9.9 9.6 14.3 16.9 9.8 7.3 10.9 13.2 8.8 7.0 17.1 5.8 6.7 9.3 9.7 12.7 12.7 11.8 8.0 4.0 4.8 6.7 9.3 9.7 12.7 12.7 12.8 8.0 7.0 17.1 5.8 6.7 9.3 9.7 12.7 12.7 12.8 12.9 12.9 12.0 12.0 12.0 12.0 12.0 12.0 12.0 12.0	84.1.8.7.7.88			
SSB	72 11.1 8.0 4.0 4.3 4.4 7.3 8.4 13.7 8.9 9.9 7.3 10.9 13.2 8.8 7.0 17.1 5.8 6.7 9.3 9.7 12.2 13.2 8.8 7.0 17.1 5.8 6.7 9.3 9.7 12.2 12.2 12.2 12.2 12.2 12.2 12.2 12	7. 7. 7. 7. 7. 7. 7. 7. 7. 7. 7. 7. 7. 7			
12	72 11.1 8.0 4.0 4.3 4.4 7.3 8.4 13.7 8.9 9.8 7.3 10.9 13.2 8.8 7.0 17.1 5.8 6.7 9.3 9.7 12.7 12.8 8.0 4.6 11.1 11.1 13.3 10.5 6.4 12.7 12.1 12.1 13.3 10.5 6.4 12.1 12.1 13.3 10.5 6.4 12.1 13.3 10.5 6.4 12.1 13.3 10.5 6.4 12.1 13.3 10.5 6.4 12.1 13.3 10.5 6.4 13.1 13.3 10.5 6.4 13.1 13.3 10.5 6.4 13.1 13.3 10.5 6.4 13.3 10.5 6.4 13.3 13.3 13.3 13.3 13.3 13.3 13.3 13	7.8.8.8.1.1.2.1.2.1.2.1.1.1.1.1.1.1.1.1.1			
See	9.9 9.6 14.3 16.9 9.8 7.3 10.9 13.2 8.8 7.0 17.1 5.8 6.7 9.3 9.7 12.7 1.8 8.0 4.6 11.1 11.1 13.3 10.5 6.4 1.1 11.1 13.3 10.5 6.4 1.2 1 11.1 11.1 13.3 10.5 6.4 1.3 10.5 6.4 1.4 11.1 11.1 11.3 10.5 6.4 1.5 2.9 11.3 7.7 8.4 6.4 1.6 3.9 0.5 0.6 10 1.8 2.0 1.7 2.0 50.5 29.2 18.7 5.1 2.4 5.3 8.1 8.0 6.9 11.7 9.4 10.2 1.1 3.4 2.2 1.6 3.8 3.9	7.0 7.0 7.0 7.0 7.0 7.0 7.0 7.0 7.0 7.0			
Sea 70 17.1 5.8 6.7 9.3 9.7 12.7 12.7 12.7 12.8 8.0 4.6 11.1 11.1 11.1 13.3 10.5 6.4 9.1 12.1 12.1 13.3 10.5 6.4 9.1 11.1 11.1 13.3 10.5 6.4 9.1 11.1 11.1 13.3 10.5 6.4 9.1 11.1 11.1 11.1 13.3 10.5 6.4 9.1 11.1 11.1 11.1 11.1 11.1 11.1 11.	8.8 7.0 17.1 5.8 6.7 9.3 9.7 12.7 12.8 8.0 4.6 11.1 11.1 13.3 10.5 6.4 12.7 12.7 12.7 12.8 12.8 12.8 12.8 12.8 12.8 12.8 12.8	2. 8 8 1. 1. 8 8 1. 1. 1. 1. 1. 1. 1. 1. 1. 1. 1. 1. 1.			
Sea 1.8 6.0 4.6 11.1 11.1 13.3 10.5 6.4 9.1 1.8 5.9 4.0 2.9 1.3 77 8.4 6.4 4.5 1.8 5.9 4.0 2.9 1.3 77 8.4 6.4 4.5 1.9 5.0 5.0 1.1 0.6 0.5 0.4 1.2 0.8 1.0 3.6 1.1 0.0 70.3 47.4 30.5 7.4 72 9.8 12.9 14.3 137 25.5 1.0 70.3 47.4 30.5 7.4 72 9.8 12.9 14.3 137 25.5 1.0 70.3 47.4 30.5 7.4 72 15.6 21.0 21.8 14.7 16.4	1.8 8.0 4.6 11.1 11.1 13.3 10.5 6.4 6.4 1.1 1.1 13.3 10.5 6.4 6.4 1.1 1.0 8.9 7.3 5.5 2.9 1.3 7.7 8.4 6.4 1.2 1.8 5.9 4.0 2.9 1.3 7.7 8.4 6.4 1.2 1.8 2.9 0.5 0.6 1.0 1.8 2.0 1.7 2.0 50.5 29.2 18.7 5.1 2.4 5.3 8.1 8.0 6.9 11.7 9.4 10.2 1.1 3.4 2.2 1.6 3.8 3.9	8 7 7 8 8 7 7 8 8 7 7 7 2 8 8 7 7 7 7 8 8 7 7 7 7 8 8 7 7 7 7			
Sselection	1.8 8.0 4.6 11.1 11.1 13.3 10.5 6.4 1.1 10.3 10.5 6.4 1.1 10.0 8.9 7.3 5.5 2.9 1.1 10 8.9 7.3 5.5 2.9 1.2 3.7 8.4 6.4 1.3 5.5 5.0 2.9 1.3 5.5 5.9 1.4 6.3 6.0 6.9 1.5 5.9 6.0 1.3 7.7 8.4 6.4 1.6 5.9 6.9 1.3 7.7 8.4 6.4 1.7 2.0 6.9 1.8 2.9 0.5 0.6 1.0 1.8 2.0 1.7 2.0 2.0 50.5 1.0 1.8 2.0 1.7 2.0 2.0 50.5 1.1 3.4 2.2 1.6 3.8 3.9	8			
ssa 1.1 1.0 8.9 7.3 5.5 2.9 6.8 1.2 1.0 8.9 7.3 5.5 2.9 6.8 1.3 7.7 8.4 6.4 4.5 1.2 1.2 1.2 1.2 1.2 1.3 1.3 1.3 1.3 1.3 1.3 1.3 1.3 1.3 1.3	1.1 1.0 8.9 7.3 5.5 2.9 1.1 1.0 8.9 7.3 6.5 2.9 1.1 2.9 1.3 7.7 8.4 6.4 1.1 2.9 0.5 0.6 1.0 1.8 2.0 1.7 2.0 50.5 29.2 18.7 5.1 2.4 5.3 8.1 8.0 6.9 11.7 9.4 10.2 1.1 3.4 2.2 1.6 3.8 3.9	2. 4. 4. 8. 4. 5. 5. 8. 4. 4. 5. 6. 6. 6. 6. 6. 6. 6. 6. 6. 6. 6. 6. 6.			
1.1 1.0 8.9 7.3 5.5 2.9 6.8 1.2 4.6 5.3 4.0 2.9 1.3 7.7 8.4 6.4 4.5 3.7 4.6 3.4 5.3 6.0 8.0 5.4 5.0 9.5 1.8 5.9 4.0 2.9 1.3 7.7 8.4 6.4 4.5 1.8 5.9 4.0 2.9 1.3 7.7 8.4 6.4 4.5 1.9 5.5 2.9 6.8 1.1 0.6 0.5 0.4 1.2 0.8 1.0 3.6 1.1 0.6 0.5 0.4 1.2 0.8 1.0 3.6 1.2 2.3 1.1 0.6 0.5 0.4 1.2 0.8 1.0 3.6 1.3 2.2 1.8 2.9 0.5 0.5 0.1 3.0 1.1 3.4 2.2 1.6 3.8 3.9 3.6 1.0 703 47.4 30.5 7.4 7.2 9.8 12.9 14.3 13.7 25.5 1.0 703 5.9 8.2 8.2 8.5 74.7 66.1 63.9 71.6 58.2 1.8 9.6 9.7 7.2 15.6 21.0 21.8 14.7 16.4	1.1 1.0 8.9 7.3 5.5 2.9 1.1 5.9 4.0 2.9 1.3 7.7 8.4 6.4 3.7 8.4 6.4 3.8 1.1 0.6 0.5 0.4 1.2 0.8 1.0 50.5 29.2 18.7 5.1 2.4 5.3 8.1 8.0 6.9 11.7 9.4 10.2 1.1 3.4 2.2 1.6 3.8 3.9	2. 5. 8. 8. 6. 7. 7. 8. 8. 6. 7. 7. 7. 7. 7. 7. 7. 7. 7. 7. 7. 7. 7.			
se 1.1 1.0 8.9 7.3 5.5 2.9 6.8 1.2 1.3 1.1 1.0 8.9 7.3 5.5 2.9 6.8 1.1 0.6 0.5 0.4 1.2 0.8 1.3 7.7 8.4 6.4 4.5 0.5 0.5 0.4 1.2 0.8 1.0 0.5 0.4 1.2 0.8 1.0 0.5 0.4 1.2 0.8 1.0 0.5 0.4 1.2 0.8 1.0 0.5 0.4 1.2 0.8 1.0 0.5 0.4 1.2 0.8 1.0 0.5 0.4 1.2 0.8 1.0 0.8 0.4 1.2 0.8 1.0 0.5 0.4 1.2 0.8 1.0 0.8 0.4 1.2 0.8 1.0 0.5 0.4 1.2 0.8 1.0 0.5 0.4 1.1 0.8 0.5 0.4 1.2 0.8 1.0 0.5 0.4 1.1 0.0 0.5 0.5 0.5 0.4 0.5 0.5 0.5 0.5 0.4 1.2 0.8 1.2 0.5 0.5 0.5 0.5 0.5 0.5 0.5 0.5 0.5 0.5	1.1 1.0 8.9 7.3 5.5 2.9 1.1 5.9 4.0 2.9 1.3 7.7 8.4 6.4 3.7 8.4 6.4 3.9 1.0 0.5 0.6 1.0 1.8 2.0 1.7 2.0 50.5 29.2 18.7 5.1 2.4 5.3 8.1 8.0 6.9 11.7 9.4 10.2 1.1 3.4 2.2 1.6 3.8 3.9	8 + 5 8 +			
1.1 10 8.9 7.3 5.5 2.9 6.8 1.2 5.9 4.0 2.9 1.3 7.7 8.4 6.4 4.5 1.3 7.7 8.4 6.4 4.5 1.4 6.3 4.6 3.4 5.3 6.0 8.0 5.4 5.0 1.5 5.5 2.9 6.8 1.6 5.9 6.8 1.1 0.6 0.5 0.4 1.2 0.8 1.0 3.6 1.7 8.4 6.3 4.6 3.4 5.3 6.0 8.0 5.4 5.0 1.8 5.9 0.5 0.5 0.5 0.4 1.2 0.8 1.0 3.6 1.9 50.5 29.2 1.8 7.5 5.6 1.0 3.8 3.9 3.6 1.0 70.3 47.4 30.5 7.4 7.2 9.8 12.9 14.3 13.7 25.5 1.8 9.6 9.7 7.2 15.6 21.0 21.8 14.7 16.4	1.1 1.0 8.9 7.3 5.5 2.9 1.1 4.0 2.9 1.3 7.7 8.4 6.4 1.1 6.3 5.8 1.1 0.6 0.5 0.4 1.2 1.8 2.9 0.5 0.6 1.0 1.8 2.0 1.7 2.0 50.5 29.2 18.7 5.1 2.4 5.3 8.1 8.0 6.9 11.7 9.4 10.2 1.1 3.4 2.2 1.6 3.8 3.9	1			
sea 1.1 1.0 8.9 7.3 5.5 2.9 6.8 1.8 5.9 4.0 2.9 1.3 77 8.4 6.4 45 3.7 4.6 3.4 5.3 6.0 8.0 5.4 5.0 9.5 18 2.9 0.5 0.5 10.7 0.8 10.2 1.3 77 8.4 6.4 45 10.0 50.5 29.2 18.7 5.1 2.4 5.3 8.1 8.0 6.9 14.1 23.8 11.7 9.4 10.2 1.1 3.4 2.2 1.6 3.8 3.9 3.6 10.0 70.3 47.4 30.5 7.4 72 9.8 12.9 14.3 13.7 25.5 10.0 70.3 47.4 30.5 7.4 72 9.8 12.9 14.3 13.7 25.5 11.8 9.6 9.7 7.2 15.6 21.0 21.8 14.7 16.4	1.1 1.0 8.9 7.3 5.5 2.9 1.2 5.9 4.0 2.9 1.3 7.7 8.4 6.4 3.7 6.3 5.8 1.1 0.6 0.5 0.4 1.2 0.8 1.0 1.8 2.9 0.5 0.6 1.0 1.8 2.0 1.7 2.0 505 292 18.7 5.1 2.4 5.3 8.1 8.0 6.9 11.7 9.4 10.2 1.1 3.4 2.2 1.6 3.8 3.9	2. 88 6. 5. 5. 7. 5. 5. 5. 5. 5. 5. 5. 5. 5. 5. 5. 5. 5.			
1.1 1.0 8.9 7.3 5.5 2.9 68 1.1 1.0 8.9 7.3 5.5 2.9 68 1.1 1.0 8.9 7.3 5.5 2.9 68 1.1 1.0 8.9 7.3 5.5 2.9 68 1.1 1.0 8.0 7.3 1.3 7.7 8.4 6.4 4.5 1.1 1.0 8.9 7.3 5.5 2.9 68 1.1 1.1 1.0 8.9 7.3 6.0 8.0 5.4 5.0 8.0 5.5 5.5 5.0 5.0 5.0 5.0 5.0 5.0 5.0 5	1.1 1.0 8.9 7.3 5.5 2.9 1.1 1.0 8.9 7.3 5.5 2.9 3.7 4.6 3.4 5.3 6.0 8.0 5.4 6.3 5.8 1.1 0.6 0.5 0.4 1.2 0.8 1.0 1.8 2.9 0.5 0.6 1.0 1.8 2.0 1.7 2.0 50.5 29.2 18.7 5.1 2.4 5.3 8.1 8.0 6.9 11.7 9.4 10.2 1.1 3.4 2.2 1.6 3.8 3.9	2. 8 4. 5. 4. 5. 4. 5. 5. 5. 5. 5. 5. 5. 5. 5. 5. 5. 5. 5.			
1.1 1.0 8.9 7.3 5.5 2.9 68 1.1 1.0 8.9 7.3 5.5 2.9 68 1.2 9 4.0 2.9 1.3 7.7 8.4 6.4 4.5 1.3 7.7 8.4 6.4 4.5 1.4 6.3 5.8 1.1 0.6 0.5 0.4 1.2 0.8 1.0 3.6 9.5 1.8 2.9 0.5 0.6 1.0 1.8 2.0 1.7 2.0 4.1 23.8 11.7 9.4 10.2 1.1 3.4 2.2 1.6 3.8 3.9 3.6 100.0 70.3 47.4 30.5 7.4 72 9.8 12.9 14.3 137 25.5 100.0 70.3 47.4 30.5 7.4 72 9.8 12.9 14.3 137 25.5 18 9.6 9.7 7.2 15.6 21.0 21.8 14.7 16.4	1.1 1.0 8.9 7.3 5.5 2.9 1.1 4.0 2.9 1.3 7.7 8.4 6.4 6.3 5.8 1.1 0.6 0.5 0.4 1.2 0.8 1.0 1.8 2.9 0.5 0.6 1.0 1.8 2.0 1.7 2.0 50.5 29.2 18.7 5.1 2.4 5.3 8.1 8.0 6.9 11.7 9.4 10.2 1.1 3.4 2.2 1.6 3.8 3.9	£ 8 + 5 + 5 + 5 + 5 + 5 + 5 + 5 + 5 + 5 +			
sea 1.1 1.0 8.9 7.3 5.5 2.9 6.8 1.1 1.0 8.9 7.3 5.5 2.9 6.8 1.2 1.8 5.9 4.0 2.9 1.3 7.7 8.4 6.4 4.5 1.2 1.8 2.9 0.5 0.6 1.0 1.8 2.0 1.7 2.0 4.1 2.0 1.7 2.0 4.1 2.0 1.7 2.0 4.1 2.0 1.7 2.0 1.7 2.0 4.1 2.0 1.7 9.4 10.2 1.1 3.4 2.2 1.6 3.8 3.9 3.6 1.0 1.0 70.3 47.4 30.5 7.4 7.2 9.8 12.9 14.3 13.7 25.5 1.8 0.0 70.3 47.4 30.5 7.4 7.2 9.8 12.9 14.3 13.7 25.5 1.8 0.0 70.3 47.4 30.5 7.4 7.2 9.8 12.9 14.3 13.7 25.5 1.8 0.0 1.0 1.0 1.0 1.0 1.0 1.0 1.0 1.0 1.0	1.1 1.0 8.9 7.3 5.5 2.9 1.2 5.9 4.0 2.9 1.3 7.7 8.4 6.4 3.7 6.3 6.0 8.0 5.4 6.3 5.8 1.1 0.6 0.5 0.4 1.2 0.8 1.0 1.8 2.9 0.5 0.6 1.0 1.8 2.0 1.7 2.0 50.5 29.2 18.7 5.1 2.4 5.3 8.1 8.0 6.9 11.7 9.4 10.2 1.1 3.4 2.2 1.6 3.8 3.9	2. 8 8 8 5 5 7 5 7 5 7 5 7 5 7 5 7 5 7 5 7			
1.1 1.0 8.9 7.3 5.5 2.9 6.8 1.2 1.8 5.9 4.0 2.9 1.3 7.7 8.4 6.4 4.5 3.7 4.6 3.4 5.3 6.0 8.0 5.4 5.0 9.5 1.8 2.9 0.5 0.6 1.0 1.8 2.0 1.7 2.0 4.1 61.9 50.5 29.2 18.7 5.1 2.4 5.3 8.1 8.0 6.9 14.1 23.8 11.7 9.4 10.2 1.1 3.4 2.2 1.6 3.8 3.9 3.6 100.0 70.3 47.4 30.5 7.4 7.2 9.8 12.9 14.3 137 2.5 5.0 100.0 70.3 47.4 30.5 7.4 7.2 9.8 12.9 14.3 137 2.5 5.0 1.8 9.6 9.7 7.2 15.6 21.0 21.8 14.7 16.4	1.1 1.0 8.9 7.3 5.5 2.9 1.3 7.7 8.4 6.4 3.7 8.4 6.4 1.1 0.6 0.5 0.6 1.0 1.8 2.0 1.7 2.0 50.5 29.2 18.7 5.1 2.4 5.3 8.1 8.0 6.9 11.7 9.4 10.2 1.1 3.4 2.2 1.6 3.8 3.9	4. 8 8 4. 5 5 5 5 4. 5 4. 5 4. 5 4. 5 4. 5 4.			
sse 1.1 1.0 8.9 7.3 5.5 2.9 6.8 1.2 5.9 4.0 2.9 1.3 7.7 8.4 6.4 4.5 2.2 1.3 5.8 1.1 0.6 0.5 0.4 1.2 0.8 1.0 3.6 9.5 1.8 2.9 0.5 0.6 1.0 1.0 8.0 5.4 5.0 9.5 1.8 2.9 1.3 7.7 8.4 6.4 4.5 9.5 1.8 2.9 1.3 7.7 8.4 6.4 4.5 1.1 0.6 0.5 0.4 1.2 0.8 1.0 3.6 9.5 1.8 2.9 1.3 7.7 8.4 6.4 4.5 9.5 1.9 1.1 0.6 0.5 0.4 1.2 0.8 1.0 3.6 1.1 0.6 0.5 1.1 3.4 2.2 1.6 3.8 3.9 3.6 100. 70.3 47.4 30.5 7.4 7.2 9.8 12.9 14.3 13.7 25.5 100. 70.3 47.4 30.5 7.4 7.2 9.8 12.9 14.3 13.7 25.5 1.8 9.6 9.7 7.2 15.6 21.0 21.8 14.7 16.4	1.1 1.0 8.9 7.3 5.5 2.9 1.8 5.9 4.0 2.9 1.3 77 8.4 6.4 3.7 4.6 3.4 5.3 6.0 8.0 5.4 6.3 5.8 1.1 0.6 0.5 0.4 1.2 0.8 1.0 50.5 29.2 18.7 5.1 2.4 5.3 8.1 8.0 6.9 11.7 9.4 10.2 1.1 3.4 2.2 1.6 3.8 3.9	5. 8.4. 5. 5. 8.5. 5. 5. 5. 5. 5. 5. 5. 5. 5. 5. 5. 5.			
1.1 1.0 8.9 7.3 5.5 2.9 6.8 1.8 5.9 4.0 2.9 1.3 7.7 8.4 6.4 4.5 3.7 4.6 3.4 5.3 6.0 8.0 5.4 5.0 4.1 61.9 50.5 2.9 6.8 1.1 0.6 0.5 0.4 1.2 0.8 1.0 3.6 5.9 6.9 5.0 5.0 5.0 5.0 5.0 5.0 5.0 5.0 5.0 5.0	1.1 1.0 8.9 7.3 5.5 2.9 1.8 5.9 4.0 2.9 1.3 7.7 8.4 6.4 3.7 4.6 3.4 5.3 6.0 8.0 5.4 6.3 5.8 1.1 0.6 0.5 0.4 1.2 0.8 1.0 1.8 2.9 0.5 0.6 1.0 1.8 2.0 1.7 2.0 50.5 29.2 18.7 5.1 2.4 5.3 8.1 8.0 6.9 11.7 9.4 10.2 1.1 3.4 2.2 1.6 3.8 3.9	2. 88 4. 5. 5. 5. 5. 5. 5. 5. 5. 5. 5. 5. 5. 5.			
ssa 1.1 1.0 8.9 7.3 5.5 2.9 6.8 1.8 5.9 4.0 2.9 1.3 7.7 8.4 6.4 4.5 3.7 4.6 3.4 6.3 6.0 8.0 5.4 5.3 9.5 1.8 2.9 0.1 1.3 7.7 8.4 6.4 4.5 9.5 1.8 2.9 0.1 1.2 7.7 8.4 6.4 4.5 9.5 1.8 2.9 0.1 1.3 7.7 8.4 6.4 4.5 9.5 1.8 2.9 1.3 7.7 8.4 6.4 4.5 9.6 1.0 1.0 1.0 1.0 1.0 1.0 1.0 1.0 1.0 1.0	1.1 1.0 8.9 7.3 5.5 2.9 1.3 7.7 8.4 6.4 3.7 8.4 6.4 1.1 0.6 0.5 0.0 1.0 1.8 2.0 1.7 2.0 50.5 29.2 18.7 5.1 2.4 5.3 8.1 8.0 6.9 11.7 9.4 10.2 1.1 3.4 2.2 1.6 3.8 3.9	2. 8.8. 2. 5.5. 2. 5.5.			
ssa 1.1 1.0 8.9 7.3 5.5 2.9 6.8 1.1 1.0 8.9 7.3 5.5 2.9 6.8 1.2 1.8 5.9 4.0 2.9 1.3 77 8.4 6.4 4.5 3.7 4.6 3.4 5.3 6.0 8.0 5.4 1.5 9.5 1.8 2.9 0.5 0.6 1.0 1.8 2.0 1.7 2.0 4.1 61.9 50.5 29.2 18.7 5.1 2.4 5.3 8.1 8.0 6.9 14.1 23.8 11.7 9.4 10.2 1.1 3.4 2.2 1.6 3.8 3.9 3.6 100.0 70.3 47.4 30.5 7.4 72 9.8 12.9 14.3 13.7 25.5 100 70.3 47.4 30.5 7.4 72 9.8 12.9 14.3 13.7 25.5 1.8 9.6 9.7 7.2 15.6 21.0 21.8 14.7 16.4	1.1 1.0 8.9 7.3 5.5 2.9 1.8 5.9 4.0 2.9 1.3 7.7 8.4 6.4 3.7 4.6 3.4 5.3 6.0 8.0 5.4 6.3 5.8 1.1 0.6 0.5 0.4 1.2 0.8 1.0 50.5 29.2 18.7 5.1 2.4 5.3 8.1 8.0 6.9 11.7 9.4 10.2 1.1 3.4 2.2 1.6 3.8 3.9	5. 8.4. 5. 5. 8.5. 5. 5. 5. 5. 5. 5. 5. 5. 5. 5. 5. 5.			
1.1 1.0 8.9 7.3 5.5 2.9 6.8 1.2 4.8 6.3 5.8 1.1 1.0 8.9 7.3 5.5 2.9 6.8 3.7 4.6 3.4 5.3 6.0 8.0 5.4 5.0 9.5 1.8 2.9 0.5 0.6 1.0 1.8 2.0 1.7 2.0 4.1 61.9 50.5 29.2 18.7 5.1 2.4 5.3 8.1 8.0 6.9 14.1 23.8 11.7 9.4 10.2 1.1 3.4 2.2 1.6 3.8 3.9 3.6 100.0 70.3 47.4 30.5 7.4 7.2 9.8 12.9 14.3 13.7 25.5 100.0 70.3 47.4 30.5 7.4 7.2 15.6 21.0 21.8 14.7 16.4	1.1 1.0 8.9 7.3 5.5 2.9 1.8 5.9 4.0 2.9 1.3 7.7 8.4 6.4 3.7 4.6 3.4 5.3 6.0 8.0 5.4 6.3 5.8 1.1 0.6 0.5 0.4 1.2 0.8 1.0 1.8 2.9 0.5 0.6 1.0 1.8 2.0 1.7 2.0 50.5 29.2 18.7 5.1 2.4 5.3 8.1 8.0 6.9 11.7 9.4 10.2 1.1 3.4 2.2 1.6 3.8 3.9	2. 88 6. 5. 5. 5. 5. 5. 5. 5. 5. 5. 5. 5. 5. 5.			
ssa 1.1 1.0 8.9 7.3 5.5 2.9 6.8 1.8 5.9 4.0 2.9 1.3 7.7 8.4 6.4 4.5 3.7 4.6 3.4 5.3 6.0 8.0 5.4 5.0 9.5 1.8 2.9 0.5 0.6 1.0 1.8 2.0 1.7 2.0 4.1 61.9 50.5 29.2 18.7 5.1 2.4 5.3 8.1 8.0 6.9 14.1 23.8 11.7 9.4 10.2 1.1 3.4 2.2 1.6 3.8 3.9 3.6 100.0 70.3 47.4 30.5 7.4 72 9.8 12.9 14.3 13.7 25.5 100 70.3 47.4 30.5 7.4 72 9.8 12.9 14.3 13.7 25.5 1.8 9.6 9.7 7.2 15.6 21.0 21.8 14.7 16.4	1.1 1.0 8.9 7.3 5.5 2.9 1.3 7.7 8.4 6.4 3.7 4.6 3.4 5.3 6.0 8.0 5.4 6.3 5.8 1.1 0.6 0.5 0.4 1.2 0.8 1.0 1.8 2.9 0.5 0.6 1.0 1.8 2.0 1.7 2.0 50.5 29.2 18.7 5.1 2.4 5.3 8.1 8.0 6.9 11.7 9.4 10.2 1.1 3.4 2.2 1.6 3.8 3.9				
ssa 1.1 1.0 8.9 7.3 5.5 2.9 6.8 1.2 1.8 5.9 4.0 2.9 1.3 77 8.4 6.4 4.5 3.7 4.6 3.4 5.3 6.0 8.0 5.4 5.0 9.5 1.8 2.9 0.5 0.4 12 0.8 1.0 36 9.5 1.8 2.9 0.5 0.6 1.0 1.8 2.0 1.7 2.0 4.1 61.9 50.5 29.2 18.7 5.1 2.4 5.3 8.1 8.0 6.9 14.1 23.8 11.7 9.4 10.2 1.1 3.4 2.2 1.6 3.8 3.9 3.6 100.0 70.3 47.4 30.5 7.4 72 9.8 12.9 14.3 13.7 25.5 100.0 70.3 47.4 30.5 7.4 72 9.8 12.9 14.3 13.7 25.5 1.8 9.6 9.7 7.2 15.6 21.0 21.8 14.7 16.4	1.1 1.0 8.9 7.3 5.5 2.9 1.8 5.9 4.0 2.9 1.3 77 8.4 6.4 3.7 4.6 3.4 5.3 6.0 8.0 5.4 6.3 5.8 1.1 0.6 0.5 0.4 1.2 0.8 1.0 50.5 29.2 18.7 5.1 2.4 5.3 8.1 8.0 6.9 11.7 9.4 10.2 1.1 3.4 2.2 1.6 3.8 3.9	4. 8 8 4 5 4 5 4 5 5 5 5 5 5 5 5 5 5 5 5 5			
1.1 1.0 8.9 7.3 5.5 2.9 6.8 1.2 5.9 4.0 2.9 1.3 7.7 8.4 6.4 4.5 2.5 2.9 6.8 2.6 4.0 2.9 1.3 7.7 8.4 6.4 4.5 3.7 4.6 3.4 5.3 6.0 8.0 5.4 5.0 3.7 4.6 0.5 0.4 1.2 0.8 1.0 3.6 3.5 29.2 18.7 5.1 0.6 0.5 0.4 1.2 0.8 1.0 3.6 4.1 0.6 0.5 0.4 1.2 0.8 1.0 3.6 4.1 0.6 0.5 0.4 1.2 0.8 1.0 3.6 4.1 0.6 0.5 0.4 1.2 0.8 1.0 3.6 4.1 0.6 0.5 0.4 1.2 0.8 1.0 3.6 4.1 0.6 0.5 0.4 1.2 0.8 1.0 3.6 4.1 0.6 0.5 0.4 1.2 0.8 1.0 3.6 4.1 0.6 0.5 0.4 1.2 0.8 1.0 3.6 4.1 0.6 0.5 0.4 1.2 0.8 1.0 3.6 4.1 0.6 0.5 0.4 1.2 0.8 1.0 3.6 4.1 0.6 0.5 0.4 1.2 0.8 1.0 3.6 4.1 0.6 0.5 0.4 1.2 0.8 1.0 3.6 4.1 0.6 0.5 0.4 1.2 0.8 1.0 3.6 4.1 0.6 0.5 0.4 1.2 0.8 1.0 2.1 1.1 3.7 25.5 4.2 0.6 0.6 0.6 0.6 0.6 0.6 0.6 0.0 3.6 4.3 0.6 0.6 0.6 0.6 0.6 0.6 0.0 3.6 4.4 0.6 0.6 0.6 0.6 0.6 0.6 0.0 3.6 4.5 0.6 0.6 0.6 0.6 0.6 0.6 0.0 3.6 4.1 0.6 0.6 0.6 0.6 0.6 0.0 3.6 4.1 0.6 0.6 0.6 0.6 0.6 0.0 3.6 4.1 0.6 0.6 0.6 0.6 0.6 0.0 3.6 4.1 0.6 0.6 0.6 0.6 0.0 3.6 4.1 0.6 0.6 0.6 0.6 0.0 3.6 4.1 0.6 0.6 0.6 0.6 0.0 3.6 4.1 0.6 0.6 0.6 0.6 0.0 3.6 4.1 0.6 0.6 0.6 0.6 0.0 3.6 4.1 0.6 0.6 0.6 0.0 3.6 4.1 0.6 0.6 0.6 0.0 3.6 4.1 0.6 0.6 0.6 0.6 0.0 3.6 4.1 0.6 0.6 0.6 0.0 3.6 4.1 0.6 0.6 0.6 0.0 3.6 4.1 0.6 0.6 0.6 0.0 3.6 4.1 0.6 0.6 0.6 0.0 3.6 4.1 0.6 0.6 0.6 0.0 3.6 4.1 0.6 0.6 0.6 0.0 3.6 4.1 0.6 0.6 0.6 0.0 3.6 4.1 0.6 0.6 0.6 0.0 3.6 4.1 0.6 0.6 0.6 0.0 3.6 4.1 0.6 0.6 0.6 0.0 3.6 4.1 0.6 0.6 0.6 0.0 3.6 4.1 0.6 0.6 0.6 0.0 3.6 4.1 0.6 0.6 0.6 0.0 3.6 4.1 0.6 0.6 0.0 3.6 4.1 0.6 0.6 0.0 3.6 4.1 0.6 0.6 0.0 3.6 4.1 0.6 0.6 0.0 3.6 4.1 0.6 0.6 0.0 3.6 4.1 0.6 0.6 0.0 3.6 4.1 0.6 0.6 0.0 3.6 4.1 0.6 0.6 0.0 3.6 4.1 0.6 0.6 0.0 3.6 4.1 0.0 0.0 3.6 4.1 0.0 0.0 3.6 4.1 0.0 0.0 3.6	1.1 1.0 8.9 7.3 5.5 2.9 1.8 5.9 4.0 2.9 1.3 7.7 8.4 6.4 3.7 4.6 3.4 5.3 6.0 8.0 5.4 6.3 5.8 1.1 0.6 0.5 0.4 1.2 0.8 1.0 1.8 2.9 0.5 0.6 1.0 1.8 2.0 1.7 2.0 50.5 29.2 18.7 5.1 2.4 5.3 8.1 8.0 6.9 11.7 9.4 10.2 1.1 3.4 2.2 1.6 3.8 3.9	2. 8. 4. 5. 5. 5. 5. 5. 5. 5. 5. 5. 5. 5. 5. 5.			
1.1 1.0 8.9 7.3 5.5 2.9 6.8 1.2 5.9 4.0 2.9 1.3 7.7 8.4 6.4 4.5 3.7 4.6 3.4 5.3 6.0 8.0 5.4 5.0 9.5 1.8 2.9 0.5 0.6 1.0 1.8 2.0 1.7 2.0 4.1 61.9 50.5 29.2 18.7 5.1 2.4 5.3 8.1 8.0 6.9 14.1 23.8 11.7 9.4 10.2 1.1 3.4 2.2 1.6 3.8 3.9 3.6 100.0 70.3 47.4 30.5 7.4 72 9.8 12.9 14.3 13.7 25.5 100.0 70.3 47.4 30.5 7.4 72 9.8 12.9 14.3 13.7 25.5 1.8 9.6 9.7 7.2 15.6 21.0 21.8 14.7 16.4	1.1 1.0 8.9 7.3 5.5 2.9 1.8 5.9 4.0 2.9 1.3 7.7 8.4 6.4 3.7 6.3 6.0 8.0 5.4 6.3 5.8 1.1 0.6 0.5 0.4 1.2 0.8 1.0 1.8 2.9 0.5 0.6 1.0 1.8 2.0 1.7 2.0 50.5 29.2 18.7 5.1 2.4 5.3 8.1 8.0 6.9 11.7 9.4 10.2 1.1 3.4 2.2 1.6 3.8 3.9	2. 8.8. 2. 5. 5. 4. 5. 5. 4. 5. 5. 4. 5. 5. 4. 5. 5. 4. 5. 5. 5. 5. 5. 5. 5. 5. 5. 5. 5. 5. 5.			
1.1 1.0 8.9 7.3 5.5 2.9 6.8 1.2 4.8 6.3 5.8 1.1 1.0 8.9 7.3 5.5 2.9 6.8 1.3 7.7 8.4 6.4 4.5 1.4 1.0 8.9 7.3 5.5 2.9 6.8 1.5 3.7 8.4 6.4 4.5 1.6 3.7 8.4 6.4 4.5 1.7 2.0 8.0 5.4 5.0 1.8 2.9 0.5 0.4 1.2 0.8 1.0 1.9 50.5 29.2 18.7 5.1 2.4 5.3 8.1 8.0 6.9 14.1 2.9 1.7 2.0 1.7 2.0 4.1 2.9 1.7 3.4 10.2 1.1 3.4 2.2 1.6 3.8 3.9 3.6 100.0 70.3 47.4 30.5 7.4 7.2 9.8 12.9 14.3 13.7 25.5 100.0 70.3 47.4 30.5 7.4 7.2 9.8 12.9 14.3 13.7 25.5 1.8 2.9 55.9 85.5 74.7 66.1 63.9 71.6 58.2 1.8 9.6 9.7 7.2 15.6 21.0 21.8 14.7 16.4	1.1 1.0 8.9 7.3 5.5 2.9 1.8 5.9 4.0 2.9 1.3 77 8.4 6.4 1.1 0.6 0.5 0.4 1.2 0.8 1.0 1.8 2.9 0.5 0.6 1.0 1.8 2.0 1.7 2.0 1.7 50.5 29.2 18.7 5.1 2.4 5.3 8.1 8.0 6.9 11.7 9.4 10.2 1.1 3.4 2.2 1.6 3.8 3.9	. 8 - 7. 2. 8 8 - 7. 2. 5. 5. 5. 5. 5. 5. 5. 5. 5. 5. 5. 5. 5.	0,4.ro, ro	رن ن د	
1.1 1.0 8.9 7.3 5.5 2.9 6.8 1.2 4.8 6.3 5.8 1.1 1.0 6.5 0.4 1.2 0.8 1.0 3.6 9.5 1.8 2.9 0.5 0.6 1.0 1.8 2.0 1.7 2.0 4.1 23.8 11.7 9.4 10.2 1.1 3.4 2.2 1.6 3.8 3.9 3.6 100.0 70.3 47.4 30.5 7.4 7.2 9.8 12.9 14.3 13.7 25.5 100.0 70.3 47.4 30.5 7.4 7.2 9.8 12.9 14.3 13.7 25.5 100.0 70.3 47.4 30.5 7.4 7.2 9.8 12.9 14.3 13.7 25.5 100.0 70.3 47.4 30.5 7.4 7.2 15.6 21.0 21.8 14.7 16.4	1.1 1.0 8.9 7.3 5.5 2.9 1.8 5.9 4.0 2.9 1.3 7.7 8.4 6.4 3.7 4.6 3.4 5.3 6.0 8.0 5.4 6.3 5.8 1.1 0.6 0.5 0.4 1.2 0.8 1.0 1.8 2.9 0.5 0.6 1.0 1.8 2.0 1.7 2.0 50.5 29.2 18.7 5.1 2.4 5.3 8.1 8.0 6.9 11.7 9.4 10.2 1.1 3.4 2.2 1.6 3.8 3.9	رن 8.4 دن 8.5 دن 1	∠1.4.r.v.a	ri O (
1.1 1.0 8.9 7.3 5.5 2.9 6.8 1.2 5.9 4.0 2.9 1.3 7.7 8.4 6.4 4.5 3.7 4.6 3.4 5.3 6.0 8.0 5.4 5.0 9.5 1.8 2.9 0.5 0.6 1.0 1.8 2.0 1.7 2.0 4.1 61.9 50.5 29.2 18.7 5.1 2.4 5.3 8.1 8.0 6.9 14.1 23.8 11.7 9.4 10.2 1.1 3.4 2.2 1.6 3.8 3.9 3.6 100.0 70.3 47.4 30.5 7.4 72 9.8 12.9 14.3 13.7 25.5 100.0 70.3 47.4 30.5 7.4 72 9.8 12.9 14.3 13.7 25.5 1.8 9.6 9.7 7.2 15.6 21.0 21.8 14.7 16.4	1.1 1.0 8.9 7.3 5.5 2.9 1.8 5.9 4.0 2.9 1.3 7.7 8.4 6.4 3.7 4.6 3.4 5.3 6.0 8.0 5.4 6.3 5.8 1.1 0.6 0.5 0.4 1.2 0.8 1.0 1.8 2.9 0.5 0.6 1.0 1.8 2.0 1.7 2.0 50.5 29.2 18.7 5.1 2.4 5.3 8.1 8.0 6.9 11.7 9.4 10.2 1.1 3.4 2.2 1.6 3.8 3.9	. 8	4 r. c. c	0.0	
1.1 1.0 8.9 7.3 5.5 2.9 6.8 1.2 1.8 5.9 4.0 2.9 1.3 7.7 8.4 6.4 4.5 3.7 4.6 0.5 0.4 1.2 0.8 1.0 3.6 9.5 1.8 2.9 0.5 0.6 1.0 1.8 2.0 1.7 2.0 4.1 61.9 50.5 29.2 18.7 5.1 2.4 5.3 8.1 8.0 6.9 14.1 23.8 11.7 9.4 10.2 1.1 3.4 2.2 1.6 3.8 3.9 3.6 100.0 70.3 47.4 30.5 7.4 72 9.8 12.9 14.3 13.7 25.5 100.0 70.3 47.4 30.5 7.4 72 9.8 12.9 14.3 13.7 25.5 1.8 9.6 9.7 7.2 15.6 21.0 21.8 14.7 16.4	1.8 5.9 4.0 2.9 1.3 7.7 8.4 6.4 6.3 5.8 1.1 0.6 0.5 0.4 1.2 0.8 0.5 5.4 50.5 29.2 18.7 5.1 2.4 5.3 8.1 8.0 6.9 11.7 9.4 10.2 1.1 3.4 2.2 1.6 3.8 3.9	8.8 1.5 1.2	ഗ്യ		
1.1 1.0 8.9 7.3 5.5 2.9 6.8 1.2 4.0 2.9 1.3 7.7 8.4 6.4 4.5 1.3 7.7 8.4 6.4 4.5 1.4 6.3 5.8 1.1 0.6 0.5 0.4 1.2 0.8 1.0 3.6 1.5 1.8 2.9 0.5 0.6 1.0 1.8 2.0 1.7 2.0 4.1 1.1 9.4 10.2 1.1 3.4 2.2 1.6 3.8 3.9 3.6 1.2 3.8 1.7 9.4 10.2 1.1 3.4 2.2 1.6 3.8 3.9 3.6 100.0 70.3 47.4 30.5 7.4 7.2 9.8 12.9 14.3 13.7 25.5 100.0 70.3 47.4 30.5 7.4 7.2 9.8 12.9 14.3 13.7 25.5 1.8 9.6 9.7 7.2 15.6 2.1.0 2.1.8 14.7 16.4	1.1 1.0 8.9 7.3 5.5 2.9 1.8 5.9 4.0 2.9 1.3 7.7 8.4 6.4 3.7 4.6 3.4 5.3 6.0 8.0 5.4 1.8 2.9 0.5 0.6 1.0 1.8 2.0 1.7 2.0 50.5 29.2 18.7 5.1 2.4 5.3 8.1 8.0 6.9 11.7 9.4 10.2 1.1 3.4 2.2 1.6 3.8 3.9	8.8 1.5 1.5	ď	9	
1.1 1.0 8.9 7.3 5.5 2.9 6.8 1.8 5.9 4.0 2.9 1.3 7.7 8.4 6.4 4.5 3.7 4.6 3.4 5.3 6.0 8.0 5.4 5.0 9.5 1.8 2.9 0.5 0.6 1.0 1.8 2.0 1.7 2.0 4.1 61.9 50.5 29.2 18.7 5.1 2.4 5.3 8.1 8.0 6.9 14.1 23.8 11.7 9.4 10.2 1.1 3.4 2.2 1.6 3.8 3.9 3.6 100.0 70.3 47.4 30.5 7.4 72 9.8 12.9 14.3 13.7 25.5 100.0 70.3 47.4 30.5 7.4 72 9.8 12.9 14.3 13.7 25.5 1.8 9.6 9.7 7.2 15.6 2.10 2.1.8 14.7 16.4	1.1 1.0 8.9 7.3 5.5 2.9 1.8 5.9 4.0 2.9 1.3 7.7 8.4 6.4 6.3 5.8 1.1 0.6 0.5 0.4 1.2 0.8 1.0 1.8 2.9 0.5 0.6 1.0 1.8 2.0 1.7 2.0 50.5 29.2 18.7 5.1 2.4 5.3 8.1 8.0 6.9 11.7 9.4 10.2 1.1 3.4 2.2 1.6 3.8 3.9	8.8 1.5 1.2	j	5	
s 4.8 6.3 5.8 1.1 1.0 8.9 7.3 5.5 2.9 6.8 6.8 4.8 6.3 5.8 1.1 0.6 0.5 0.4 1.2 0.8 1.0 3.6 5.9 5.0 5.0 5.0 5.0 5.0 5.0 5.0 5.0 5.0 5.0	1.8 5.9 4.0 2.9 7.3 5.5 2.9 3.7 4.6 3.4 5.3 6.0 8.0 5.4 6.3 5.8 1.1 0.6 0.5 0.4 1.2 0.8 1.0 1.8 2.9 0.5 0.6 1.0 1.8 2.0 1.7 2.0 50.5 29.2 18.7 5.1 2.4 5.3 8.1 8.0 6.9 11.7 9.4 10.2 1.1 3.4 2.2 1.6 3.8 3.9	8.8 1.5 12.1			
1.8 5.9 4.0 2.9 1.3 7.7 8.4 6.4 4.5 3.7 4.6 3.4 5.3 6.0 8.0 5.4 5.0 5.0 5.0 5.0 5.0 5.0 5.0 5.0 5.0 5.0	1.8 5.9 4.0 2.9 1.3 7.7 8.4 6.4 8.3 8.1 8.0 8.0 5.4 8.4 8.4 8.4 8.4 8.3 8.0 8.0 5.4 8.4 8.4 8.4 8.4 8.4 8.4 8.4 8.4 8.4 8	12.15			
s 4.8 6.3 5.8 4.0 2.9 1.3 7.7 8.4 6.4 4.5 3.6 6.3 5.8 6.3 8.0 5.4 5.0 8.0 8.0 5.4 5.0 8.0 8.0 5.4 5.0 8.0 8.0 5.4 5.0 8.0 8.0 5.4 5.0 8.0 8.0 5.4 5.0 8.0 8.0 5.4 5.0 8.0 8.0 5.4 5.0 8.0 8.0 5.0 8.0 8.0 5.4 5.0 8.0 8.0 8.0 8.0 8.0 8.0 8.0 8.0 8.0 8	1.8 5.9 4.0 2.9 1.3 7.7 8.4 6.4 6.3 5.8 1.1 0.6 0.5 0.4 1.2 0.8 1.0 1.8 2.9 0.5 0.6 1.0 1.8 2.0 1.7 2.0 50.5 29.2 18.7 5.1 2.4 5.3 8.1 8.0 6.9 11.7 9.4 10.2 1.1 3.4 2.2 1.6 3.8 3.9	12.1			
s 4.8 6.3 5.8 4.0 2.9 1.3 7.7 8.4 6.4 4.5 5.0 5.0 5.0 5.0 5.0 5.0 5.0 5.0 5.0 5	1.8 5.9 4.0 2.9 1.3 7.7 8.4 6.4 3.7 8.4 6.4 6.4 8.2 6.3 5.8 1.1 0.6 0.5 0.4 1.2 0.8 1.0 5.0 5.0 5.0 5.0 5.0 5.0 5.0 5.0 5.0 5	12.1			
3.7 4.6 3.4 5.3 6.0 8.0 5.4 5.0 8.0 8.4 5.0 8.0 8.4 5.0 8.0 8.4 5.0 8.0 8.4 5.0 8.0 8.4 5.0 8.0 8.4 5.0 8.0 8.4 5.0 8.0 8.4 5.0 8.0 8.0 8.4 5.0 8.0 8.0 8.4 8.0 8.0 8.4 8.0 8.0 8.0 8.0 8.0 8.0 8.0 8.0 8.0 8.0	3.7 4.6 3.4 5.3 6.0 8.0 5.4 1.0 6.3 5.4 1.1 0.6 0.5 0.4 1.2 0.8 1.0 1.0 1.8 2.9 0.5 0.6 1.0 1.8 2.0 1.7 2.0 5.5 29.2 18.7 5.1 2.4 5.3 8.1 8.0 6.9 11.7 9.4 10.2 1.1 3.4 2.2 1.6 3.8 3.9				
4.8 6.3 5.8 1.1 0.6 0.5 0.4 1.2 0.8 1.0 3.6 9.5 1.8 2.9 1.0 3.6 1.0 3.6 9.5 1.8 2.9 0.5 0.6 1.0 1.8 2.0 1.7 2.0 4.1 21.8 1.7 2.0 4.1 2.1 2.3 8.1 8.0 6.9 14.1 2.3 8.1 8.0 6.9 14.1 3.8 3.9 3.6 1.0 1.0 70.3 47.4 30.5 7.4 7.2 9.8 12.9 14.3 13.7 25.5 3.9 3.6 1.8 9.6 9.7 7.2 15.6 2.1 0.2 2.8 14.7 16.4 16.4	6.3 5.8 1.1 0.6 0.5 0.4 1.2 0.8 1.0 1.8 2.9 0.5 0.6 10 1.8 2.0 1.7 2.0 50.5 29.2 18.7 5.1 2.4 5.3 8.1 8.0 6.9 11.7 9.4 10.2 1.1 3.4 2.2 1.6 3.8 3.9	17.3 12			
9.5 1.8 2.9 0.5 0.6 1.0 1.8 2.0 1.7 2.0 4.1 61.9 50.5 29.2 18.7 5.1 2.4 5.3 8.1 8.0 6.9 14.1 23.8 11.7 9.4 10.2 1.1 3.4 2.2 1.6 3.8 3.9 3.6 10.0 70.3 47.4 30.5 7.4 72 9.8 12.9 14.3 13.7 25.5 30.0 50.9 59.9 85.5 74.7 66.1 63.9 71.6 58.2 16.4 10.4 10.5 10.0 70.3 47.4 30.5 7.4 72 9.8 12.9 14.3 13.7 25.5 10.0 50.9 59.9 82.9 85.5 74.7 66.1 63.9 71.6 58.2 10.0 21.8 14.7 16.4	1.8 2.9 0.5 0.6 1.0 1.8 2.0 1.7 2.0 50.5 29.2 18.7 5.1 2.4 5.3 8.1 8.0 6.9 11.7 9.4 10.2 1.1 3.4 2.2 1.6 3.8 3.9	0.4			
61.9 50.5 29.2 18.7 5.1 2.4 5.3 8.1 8.0 6.9 14.1 23.8 11.7 9.4 10.2 1.1 3.4 2.2 1.6 3.8 3.9 3.6 14.1 100.0 70.3 47.4 30.5 7.4 7.2 9.8 12.9 14.3 13.7 25.5 29/lob/gerina 29.7 50.9 59.9 82.9 85.5 74.7 66.1 63.9 71.6 58.2 1.8 9.6 9.7 7.2 15.6 21.0 21.8 14.7 16.4	50.5 29.2 18.7 5.1 2.4 5.3 8.1 8.0 6.9 11.7 9.4 10.2 1.1 3.4 2.2 1.6 3.8 3.9	0.7			
23.8 11.7 9.4 10.2 1.1 3.4 2.2 1.6 3.8 3.9 3.6 3.9 3.6 10.0 70.3 47.4 30.5 7.4 7.2 9.8 12.9 14.3 13.7 25.5 10.0 50.9 59.9 82.9 85.5 74.7 66.1 63.9 71.6 58.2 1.8 9.6 9.7 7.2 15.6 21.0 21.8 14.7 16.4	11.7 9.4 10.2 1.1 3.4 2.2 1.6 3.8 3.9	5.5			
100.0 70.3 47.4 30.5 7.4 7.2 9.8 12.9 14.3 13.7 25.5 Oglobigerina 29.7 50.9 59.9 82.9 85.5 74.7 66.1 63.9 71.6 58.2 1.8 9.6 9.7 7.2 15.6 21.0 21.8 14.7 16.4		2.2	2.5 1.9	.9 2.9	4.2 0.3
100.0 70.3 47.4 30.5 7.4 7.2 9.8 12.9 14.3 13.7 25.5 Oglobigerina 29.7 50.9 59.9 82.9 85.5 74.7 66.1 63.9 71.6 58.2 1.8 9.6 9.7 7.2 15.6 21.0 21.8 14.7 16.4					
100.0 70.3 47.4 30.3 7.4 7.2 3.0 12.9 14.3 13.7 25.3 29/lobigerina 29.7 50.9 59.9 82.9 85.5 74.7 66.1 63.9 71.6 58.2 1.8 9.6 9.7 7.2 15.6 21.0 21.8 14.7 16.4		c			
ograngerina 29.1 30.3 35.3 74.1 30.1 33.9 71.0 30.2 1.1 16.4 14.7 16.4 16.4 17.1 16.4 17.1 16.4 17.1 16.4 17.1 16.4 17.1 16.4 17.1 16.4 17.1 16.4 17.1 17.1 17.1 17.1 17.1 17.1 17.1 17	100.0 10.3 47.4 30.3 7.4 7.2 9.6 12.9 14.3 15.7 23	0 0			0.0
1,8 9,0 8,7 7,2 15,0 21,0 21,8 14,7 10,4	28.7 50.9 58.9 62.9 65.5 74.7 66.1 63.9 71.0 56 19 06 07 73 156 510 519 147 16	v =	26.9 5.0	0. c	
	0.12 0.12 0.00 2.1	. r			
r arabibouna Praemurica Globoconusa					
r aemulica Globoconusa		0.2			
		0.8			3.1 1.8 0.6
Total automotion and 111 171 107 17E 010 020 001 000	CO 111 171 107 17E 007 000 000		040	270	010

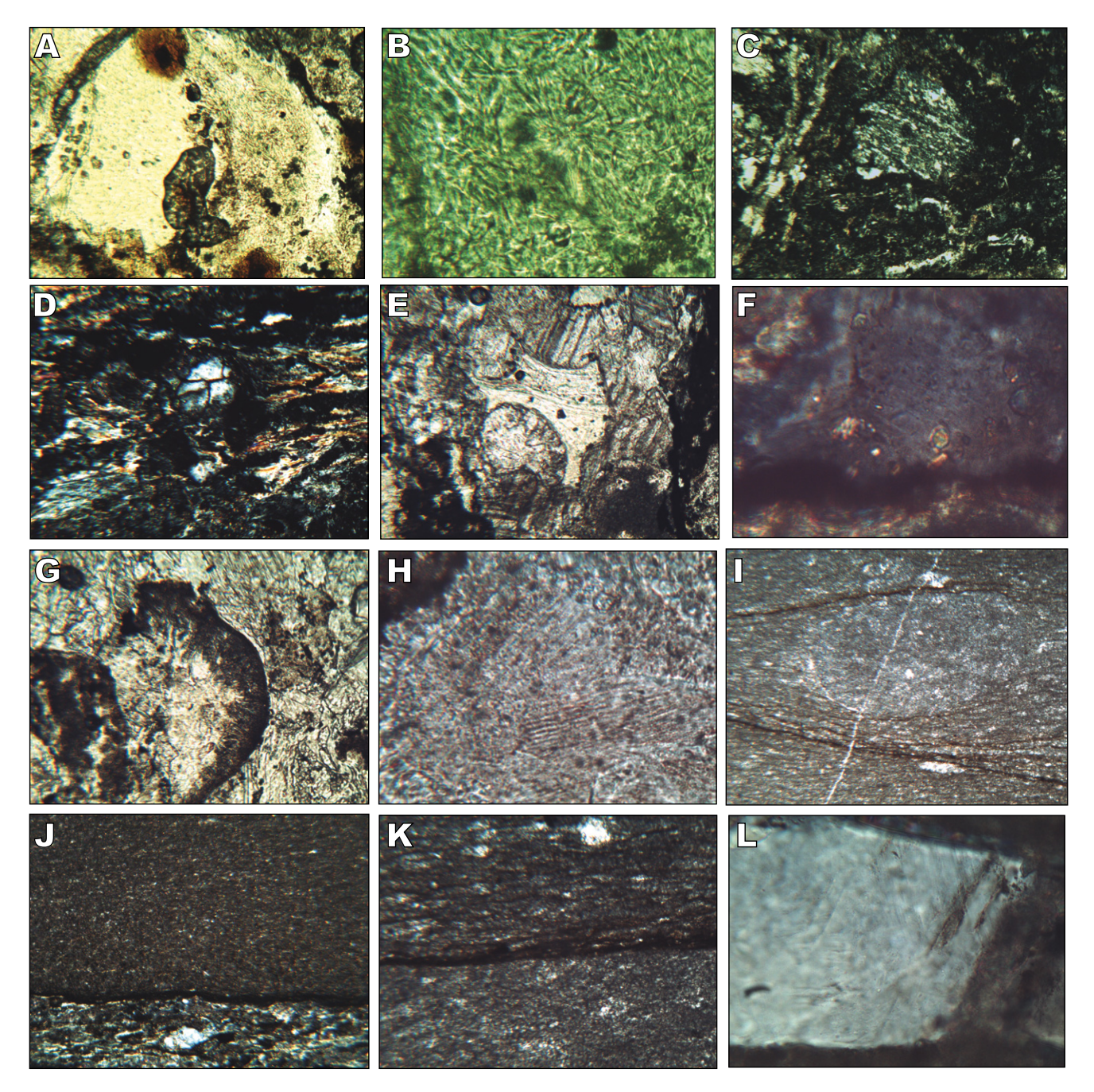


FIGURE 5. Petrographic images of polished thin sections from the main units of Moncada section. A) Altered-devitrified glass fragment with quench texture (photomicrograph is 600μm across, plane-polarized light), basal part of the Moncada Fm. (lower Unit 1). B) Detail of A, illustrating the quench texture of the altered glass fragment (photomicrograph is 160μm across, plane-polarized light), basal part of the Moncada Fm. (lower Unit 1). C) Schist clast included in melt rock fragment (photomicrograph is 2.4mm across, crossed-polarized light), basal part of the Moncada Fm. (lower Unit 1). D) Flow-textured ejecta with quartz, sericite and muscovite (photomicrograph is 600μm across, crossed-polarized light, lower part of the Moncada Fm. (upper Unit 1). E) Smectite shards and calcite filled bubble from a broken spherule (photomicrograph is 600μm across, plane-polarized light), lower part of the Moncada Fm. (upper Unit 1). G) Broken smectite altered spherule with radiating pyroxene crystals (photomicrograph is 600μm across, plane-polarized light), middle part of the Moncada Fm. (Unit 3). H) Shocked quartz grain showing at least two set of PDFs (photomicrograph is 155μm across, plane-polarized light), upper part of the Moncada Fm. (Unit 4). I) Lime mudstone showing burrowing-like structures and dark clay lamination (photomicrograph is 2.4mm across, crossed-polarized light), dark clayey mudstone bed or "K/T boundary clay" (UMU-1, *H. holmdelensis* subzone). J) Contact between medium-sand sized ejecta below and clayed micrite above (photomicrograph is 600μm across, crossed-polarized light), contact between uppermost part of the Moncada Fm. (Unit 5) and UMU-1. K) Lime mudstone showing numerous clay lamination (photomicrograph is 600μm across, plane-polarized light), dark clayey mudstone bed or "K/T boundary clay" (UMU-1). L) Shocked quartz grain. Detail from reworked shocked quartz grain in clayey micritic limestone to show PDFs, (photomicrograph is 160μm across, plane-polarized light), basal part of Ancón Fm. (*Pv. long*

of melt rock clasts (Fig. 5D), smectite spherules and smectite shards (Fig. 5E), quartz grains, and scarce micritic limestone fragments. The diameter of the grains fluctuates from 0.6 to 0.9mm, intermediate sizes being more abundant. The matrix is mainly composed of sericite and smectite as the alteration product of glass fragments. Due to subsequent low-grade metamorphic processes muscovite and sericite flakes are abundant in this sample. Bubbles in smectite spherule are filled with spatic calcite. Some quartz grains that seem to be igneous or metamorphic in origin have parallel or undulant extinction, but other grains show impact effects such as Planar Deformation Features (PDFs) and/or features of roasting (Fig. 5F).

The middle part of the Moncada Fm. (U2) corresponds to medium sand-sized ejecta material with a flow-like banded texture. It is composed of melt rock fragments, calcite and smectite spherules and shards (Fig. 5G), and quartz, bound together by a matrix consisting of calcite, sericite, smectite, and minor amounts of chlorite, produced by the alteration of glass. Like other samples from the lower part, the ejecta grain size varies from 0.1 to 1mm.

The upper part of the Moncada Fm. (U4) also corresponds to fine to medium sand-sized (0.1 to 0.8mm) ejecta with no orientation of the grains. In equal proportions, the matrix is composed of recrystallized micrite and smectite spherule fragments and shards. The alteration minerals are mainly smectite, calcite and minor chlorite. The matrix encloses altered melt rock, glass, shards, quartz and minor amounts of pyroxene and biotite fragments. The quartz (0.1 to 0.2mm) from the upper part preserves planar microstructures (Fig. 5H).

The 2cm thick clayey lime mudstone in the uppermost part of the Moncada Fm. (UMU-1) is characterized by the presence of several very thin clay laminations and some burrow structures (Fig. 5I). The contact between the upper part of the ejecta-rich CCU and the overlying clayey UMU-1 is marked by a tiny, 30-50 µm thick layer of dark clay. The ejecta material below this dark clay (Fig. 5J), which corresponds to the CCU (uppermost part of U5), is constituted by melt rock fragments, broken calcite/ smectite spherules, quartz grains and dispersed smectite and calcite crystals. The 1cm thick UMU-2 is characterized by medium to fine sand-sized ejecta (0.1 to 0.7mm) with a roughly flow-like texture. Its matrix is composed of smectite resulting from the alteration of glass fragments and shards, and abundant calcite. This smectite-calcite matrix encloses altered melt rock, glass, shards and quartz fragments.

Tada *et al.* (2002) found a high Ir concentration not only in UMU-1, but also in the 1cm thick yellowish marly limestone at the base of the Ancón Fm. The Ir concentration

remains relatively high in the first 5 centimeters of the Ancón Fm., *i.e.*, throughout the entire *G. cretacea* zone. This stratigraphic interval corresponds to lime mudstone with several quartz grains, microfossils and widespread micron-sized dark clay laminations (Fig. 5K). The majority of the quartz grains lack impact features, but others show planar microstructures probably related to shock metamorphism (Fig. 5L).

Evidence from planktonic foraminifera

To help with the micropaleontological identification and dating of the CCU in the Gulf of Mexico and the Caribbean, Arenillas et al. (2011) described several planktonic foraminiferal markers of the K/Pg boundary based on high-resolution biostratigraphic studies of the most continuous Tethyan sections such as El Kef (see Arenillas et al., 2004; Molina et al., 2006, 2009). i) Identification of the P. hantkeninoides zone in the uppermost part of Cretaceous deposits, since this is the highest biozone of the Maastrichtian in tropical-subtropical latitudes, with an estimated duration of ~300kyr, and its top coincides with the K/Pg boundary mass extinction of planktonic foraminifera. ii) Identification of reworked specimens of P. hantkeninoides and/or other end-Cretaceous species (e.g., Abathomphalus mayaroensis, Pseudoguembelina hariaensis, or Racemiguembelina fructicosa) within the CCU, corroborating the hypothesis that eroded uppermost Maastrichtian sediments accumulated in the local CCU. iii) Identification of zone P0 or H. holmdelensis subzone, since this biozone spans approximately the first 6kyr of the Danian, and its identification above the CCU confirms that the latter is related to the K/Pg boundary. iv) Identification of PFAS 1, since this is the first planktonic foraminiferal acme-stage recorded in the Danian above the K/Pg boundary, with an estimated duration of 10 to 12kyr, and it is a particularly interesting K/Pg marker because it minimizes potential taxonomic problems in the species assignments.

Biostratigraphic markers 1, 3 and 4 allow direct identification of the K/Pg boundary, while marker 2 allows only indirect identification, because it is based on reworked specimens. The identification of markers 1, 3 and 4 does not necessarily imply the absence of stratigraphic hiatuses at the top of the Cretaceous and/or at the base of the Paleogene. However, their identification implies that such hiatuses, if there are any, affect only small intervals of time on a geological scale.

In the upper part of the Cretaceous deposits of the Pons Fm., only *Favusella washitensis*, *Heterohelix moremani*? and *Hedbergella sigali* have been identified in the disaggregated samples analyzed (Fig. 2). According to Caron (1985), the presence of these species suggests that

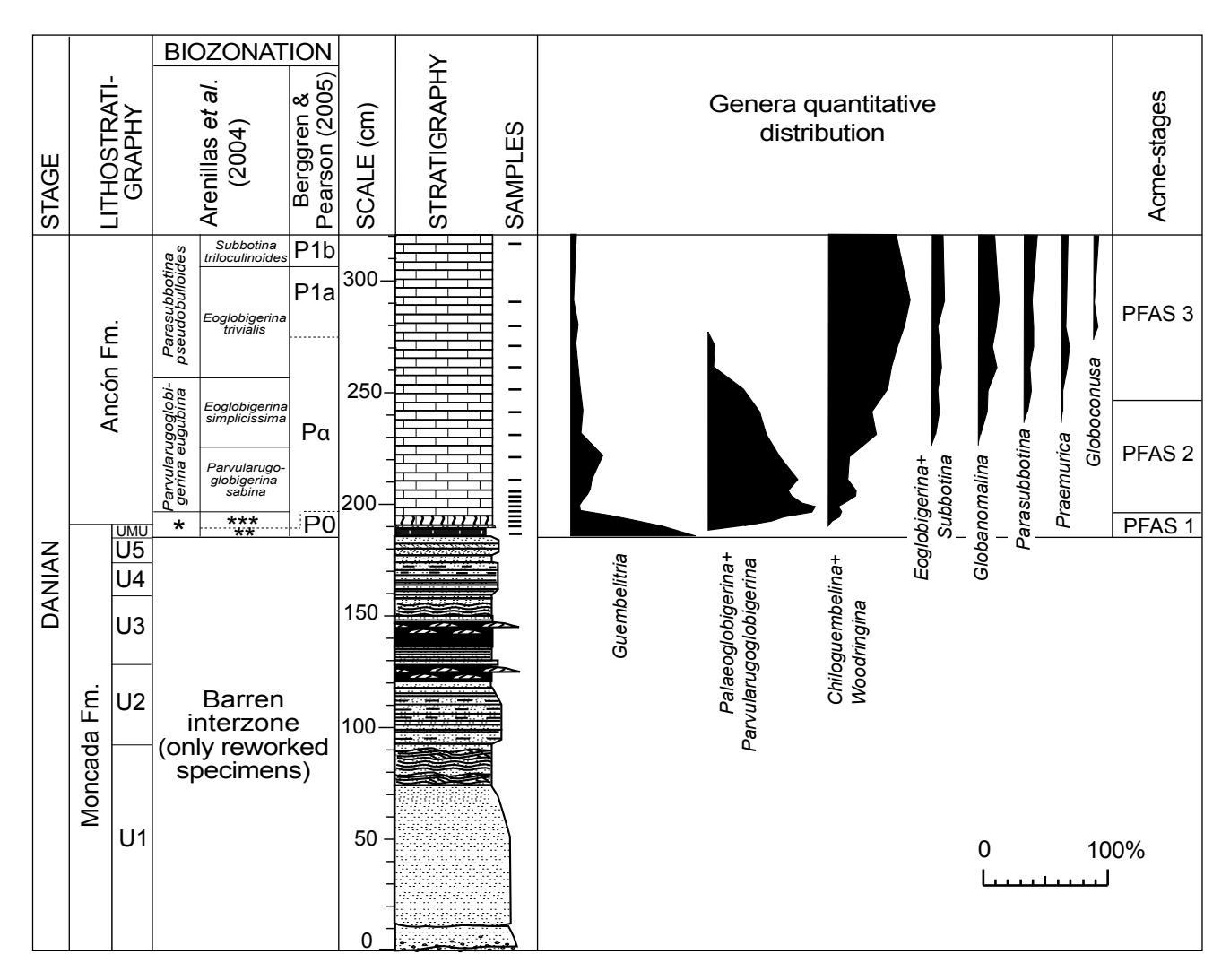


FIGURE 6. Relative abundance of Planktonic Foraminiferal genera and Acme Stages (PFAS) in the lowermost Danian of the Moncada section. *Guembelitria cretacea zone, *** Hedbergella holmdelensis subzone, *** Parvularugoglobigerina longiapertura subzone.

the top of the Pons Fm. at Moncada is Albian in age, but it is not possible to determine to which biozone it belongs. It suggests a significant erosional hiatus between the Pons Fm. and the Moncada Fm. affecting all the Upper Cretaceous rocks. Similar erosional unconformity related to the deposition of the CCU has been identified recently in several wells from the north-central Gulf of Mexico (Scott et al., 2014), making it nearly impossible to use marker 1 in this region. The amount of time represented by these hiatuses in different sections is variable, but on average it increases in magnitude with proximity to the impact site, i.e., the Chicxulub crater (Arenillas et al., 2011).

The clastic nature and sedimentary structures of the Moncada Fm. indicate that it only contain reworked and mixed foraminiferal assemblages, so this stratigraphical interval cannot be assigned to any biozone and is included in a barren interzone (Fig. 2). Nevertheless, reworked specimens have

allowed us to analyze the age of the material eroded, transported and redeposited in the Moncada Fm. In this formation, we have only been able to recognize poorly preserved planktonic foraminiferal specimens of *Pseudotextularia nuttalli*, *Racemiguembellina fructicosa*, *Gansserina gansseri*, *Globotruncanita fareedi* and *Globotruncana arca*. In particular, the presence of *R. fructicosa* suggests that part of the carbonate material deposited in the Moncada Fm. is Maastrichtian in age (marker 2).

At Moncada, the six lowermost Danian subzones of the Arenillas *et al.* (2004) zonation were identified above the CCU, *i.e.*, in the UMU and the Ancón Fm. (Figs. 2; 3; 6). This complete planktonic foraminiferal biostratigraphic sequence as well as the identification of the *H. holmdelensis* subzone or zone P0 (marker 3) corroborate that the underlying CCU, *i.e.*, the Moncada Fm., is K/Pg in age. The *H. holmdelensis* subzone contains oligotaxic planktonic

foraminiferal assemblages composed only of *Guembelitria* species. We highlight the lack of other species deriving from the Cretaceous, such as *Heterohelix globulosa*, *Hedbergella holmdelensis* and *H. monmouthensis*, generally considered survivors of the K/Pg mass extinction and usually present in zone P0 worldwide (see Olsson *et al.*, 1999; Molina *et al.*, 2006, 2009; and references quoted there). Except for *Guembelitria* species, there is also no Cretaceous species in the *Pv. longiapertura* subzone.

The sequence of PFAS of Arenillas *et al.* (2006) is also recognizable in the lower Danian of the Moncada section (Fig. 6). PFAS-1 or the *Guembelitria* acme includes the UMU and the first 1.5 centimeters of the Ancón Fm. Reworking and infiltration processes due to the bioturbation in the Ancón Fm., mainly in its basal part, may have altered the relative abundances of the planktonic foraminifera taxa, but the PFAS sequence also confirms the stratigraphic continuity of the lower Danian between the Moncada and Ancón formations. Although minor stratigraphic hiatuses may exist between the different units (CCU, UMU-1, UMU-2 and Ancón Fm.), no significant hiatus is biostratigraphically recognizable in the lower Danian of the Moncada outcrop.

DISCUSSION

Age of the Moncada Formation and the Chicxulub impact

The Global boundary Stratotype Section and Point (GSSP) of the base of the Danian, or the K/Pg boundary, was defined at the base of the bed informally known as the "K/T Boundary Clay" in the El Kef section, Tunisia, specifically at the base of a 2-5mm thick Ir-rich layer that contains a peak of Ni-rich spinels and coincides with the catastrophic mass extinction of planktonic foraminifera (Molina et al., 2006). This definition implies that the impact-generated sediments in the K/Pg boundary belong chronostratigraphically to the Danian (Arz et al., 2004; Molina et al., 2009; Schulte et al., 2010). The "K/T Boundary Clay" in continuous sections of the Tethyan region is composed of two beds (Arenillas et al., 2011). i) A millimeter-thick ejecta-rich airfall layer, usually reddish, with high concentrations of Ir (the wellknown Ir anomaly); Arenillas et al. (2006) showed that the Chicxulub-related CCU in the Gulf of Mexico and Caribbean sections is synchronous with this airfall layer and the K/Pg catastrophic mass extinction horizon in the Tethyan sections. ii) A dark clay bed with low values in δ^{13} C, spanning the *H. holmdelensis* subzone (*i.e.*, zone P0) and the lowermost part of the Pv. longiapertura subzone (*i.e.*, lowermost part of zone $P\alpha$).

According to this description, we can draw two relevant conclusions at Moncada. i) Mineralogical and petrographic

evidence indicates that U1 to U5 of the Moncada Fm. are isochronous with the K/Pg millimeter-thick ejecta-rich airfall layer, and the K/Pg boundary should be placed at the base of this formation. Since the deposition of the Moncada Fm. is linked to the Chicxulub impact event, the latter is also K/Pg in age. ii) Micropaleontological evidence indicates that UMU-1 represents the "K/T Boundary Clay" at Moncada, specifically the dark clay bed. The planktonic foraminiferal assemblages are composed exclusively of *Guembelitria* species, therefore belonging to zone P0 and the acme-stage PFAS-1 (markers 3 and 4 respectively). This clayey subunit is truncated by the sandy UMU-2, which is a thin turbiditic layer whose deposition is temporarily disconnected from that of the CCU.

It is important to notice that these biostratigraphic results are similar to those reported from the Bochil and Guayal sections, southwestern Mexico, where the "K/T Boundary Clay" is 5 and 3 centimeters thick respectively (Arenillas et al., 2006). As at Moncada, the lowermost Danian zone P0 or the H. holmdelensis subzone and PFAS-1 were also identified in a dark clay bed just above the CCU, proving that such a bed is chronostratigraphically equivalent to the "K/T Boundary Clay" of the El Kef section (Fig. 7). In the southwestern Mexican sections, the CCU exhibits four subunits (Grajales-Nishimura et al., 2003). i) Subunit 1 consists of very coarse-grained carbonate breccia, with clasts composed predominantly of facies with shallowwater taxa (e.g., rudist fragments); the breccia matrix contains reworked Maastrichtian foraminifera specimens (such as Pseudoguembelina hariaensis). ii) Subunit 2 consists of coarse-grained sandstone with shocked quartz and spherules. iii) Subunit 3 consists of fine-grained sandstone and siltstone with shocked materials, spherules and accretionary lapilli. iv) Subunit 4 consists of a thin yellow-red shaly layer and shows a distinctive Ir anomaly, 1.5ppb at Bochil and 0.8ppb at Guayal at the top of their CCU, and it represents the finest ejecta (Montanari et al., 1994; Tagle and Claeys, 2001).

Despite being relatively near the Chicxulub impact site, the Moncada section, unlike Bochil and Guayal sections, contains no breccia subunit (Subunit 1) in the lower part of its CCU. This absence suggests that the landslides and probably the action of megatsunamis triggered by the Chicxulub impact prevented the deposition of breccia in the uppermost slope of the eastern Yucatan peninsula (see Fig. 1), where Moncada was located (Tada *et al.*, 2003). The uppermost subunits (2 to 4) of the CCU in the southwestern Mexican sections are equivalent to those found in the Moncada Fm. (Fig. 7). All this evidence supports the theory that the Chicxulub impact occurred just at the K/Pg boundary, and triggered the catastrophic mass extinction event as well as severe short and long-term paleoenvironmental effects (Schulte *et al.*, 2010).

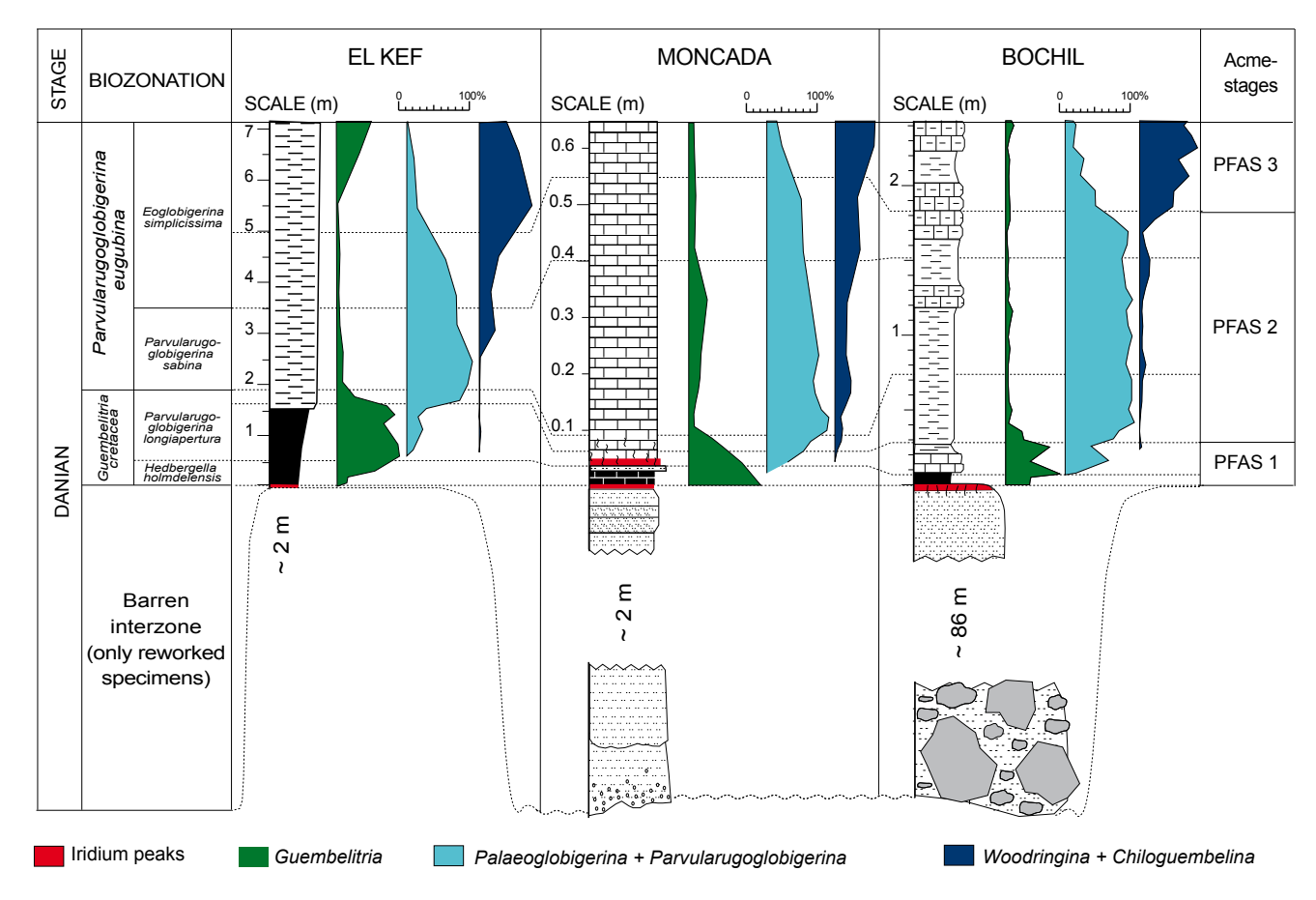


FIGURE 7. Comparison of relative abundance of Planktonic Foraminiferal Groups and Acme Stages (PFAS) in the lowermost part of the Danian at El Kef, Moncada and Bochil.

This conclusion agrees with Renne *et al.* (2013), who have precisely determined the age of the Chicxulub impact by performing ⁴⁰Ar/³⁹Ar dating on Haitian tektites and on sanidine from bentonites clearly associated with the K/Pg boundary in Montana, USA. These ⁴⁰Ar/³⁹Ar data show the synchrony between the K/Pg boundary extinction event and the Chicxulub impact to within 32Kyr, countering the hypothesis that the latter predated the K/Pg boundary by ~300kyr.

One or two iridium anomalies?

The high Ir concentration throughout the UMU and the first centimeters of the Ancón Fm. at Moncada, *i.e.*, across the *G. cretacea* zone, seems to contradict the event sequence identified in the Tethyan sections, where the Ir peak is mainly concentrated in the millimeter-thick airfall layer equivalent to the CCU in the Gulf of Mexico and the Caribbean region. However, it is well known that iridium is easily mobilized by diffusion through the sediments (Colodner *et al.*, 1992; Lee *et al.*, 2003; Morgan *et al.*, 2006), which could partly explain its high concentration in the lowermost Danian of Moncada. Bioturbation processes, recognizable in the UMU and the basal part of the Ancón

Fm., could have also contributed to its dispersion by reworking across the *G. cretacea* zone. Furthermore, the high Ir concentration in this biozone could also be the result of the progressive contribution of ejecta material from shallower environments for thousands of years after the K/Pg impact, as suggested by the presence of the ejecta-rich clay laminations in the lowermost part of the Ancón Fm.

Quartz grains with planar microstructures, micronsized dark clay laminations, intimate clay-lime mud associations, and burrow structures observed in the lime mud of the first 5 centimeters of the Ancón Fm. (Fig. 5I, J, K) suggest two sedimentary processes during the earliest Danian of Moncada after the Chicxulub impact. i) A sedimentary mixing process by bioturbation. ii) Erosion and destabilization of the CCU in higher topographic levels (e.g., on land and/or shallow shelves), probably by severe storms and/or earthquakes, giving rise to normal turbidite flows as well as the re-suspension of Ir-rich, clayey ejecta material, and its re-sedimentation in deeper locations such as Moncada. Both these sedimentary processes mixed the autochthonous marine lime mud and the reworked/resuspended ejecta that fell into the basin in the Moncada area. The greatest proportions of re-suspended ejecta occur in the UMU-1 claystone and the Ir-rich yellowish marly limestone of the basal part of the Ancón Fm. reported by Tada *et al.* (2002). Smit and Romein (1985) proposed a similar scenario at Deep Sea Drilling Project (DSDP) Site 577 (Shatsky Rise, North Pacific), in which enhanced Ir levels in *G. cretacea* and *Pv. eugubina* zones are probably either due to bioturbation/reworking or to erosion and redeposition from other eroded fall-out deposits, *e.g.*, on land. Higher concentrations of iridium in the lowermost Danian have also been identified in other Gulf of Mexico localities, such as El Mimbral, northeastern Mexico (Smit *et al.*, 1996).

Short and long-term paleoenvironmental effects of the Chicxulub impact

Pollution by re-suspended particles and contaminant elements probably contributed to stressful ecological conditions worldwide for thousands of years after the K/ Pg boundary and influenced the evolution of planktonic foraminifera in the earliest Danian. Poisoning by heavy metals, ejected from the impact site (i.e., Chicxulub), may have provided long-term mechanisms of environmental stress for plankton. Calculations of trace element fluxes to the ocean associated with a hypothetical 10kmdiameter Chicxulub impactor indicate that the mass of heavy metals contained in the bolide, such as Co, Ni, Cu and Hg, are comparable to or larger than the world ocean burden (Erickson and Dickson, 1987). According to these authors, heavy metals with relatively inefficient removal mechanisms, such as Cu and Ni with greater than 1000yrs steady-state oceanic residence time, would have mixed throughout the entire volume of the ocean. Later, the worldwide sediments contaminated with heavy metals, including Ir and other platinoids, could have been eroded, removed and re-suspended in oceans for a long time (Smit and Romein, 1985; Smit et al., 1996). Enhanced levels of toxic heavy metals (e.g., Ni, Zn, Cr, or Cu) have been identified in G. cretacea and Pv. eugubina zones (mainly in the "K/T Boundary Clay", i.e., the first 10kyr after the K/Pg boundary), even in distant localities from Chicxulub as Aïn Settara, Tunisia (Dupuis et al., 2001), and Stevns Klint, Denmark (Premovic et al., 2008).

The action of these pollutants must have been very intense just after the Chicxulub impact (Erickson and Dickson, 1987) and was probably one of the paleoenvironmental factors that caused the K/Pg boundary mass extinction of planktonic foraminifera, along with the short-lived global cooling during the "impact winter" (see Vellekoop *et al.*, 2014), the breakdown of food chains and the productivity collapse (see Aberhan *et al.*, 2007), and the acidification of the ocean surface (see Alegret *et al.*, 2011). The real aftermath of the contaminants of meteoritic origin and other paleoenvironmental factors

on the planktonic foraminiferal assemblages remains to be evaluated, but the Moncada section may provide some hints. Except for Guembelitria species, the absence of cosmopolitan, generalist Cretaceous species, such as Heterohelix globulosa, Hedbergella holmdelensis and Hedbergella monmouthensis (Petrizzo, 2002), in the UMU and the basal part of the Ancón Fm. is remarkable. The low abundance of planktonic foraminifera in this stratigraphic interval and the poor preservation prevents a better test in Moncada, but the lack of these Cretaceous species cannot be attributed only to taphonomical/diagenetic factors because, although poorly preserved, planktonic foraminifera species with small and thin tests have been identified in the same levels. By contrast, Cretaceous species are frequent in the lowermost part of the Danian, mainly in zone P0, in most continuous K/Pg sections of the Gulf of Mexico and the Tethys (see Molina et al., 2006, 2009). Given the new evidence from the Moncada section, it would be reasonable to argue that, except for guembelitrids, the presence of Cretaceous species within the lowermost Danian at most K/Pg localities may be the result of normal reworking/ bioturbation processes worldwide (see Huber 1996; Kaiho and Lamolda, 1999; Rodríguez-Tovar et al., 2010).

The Cretaceous rocks from the main source area of the clastic material of the Moncada and Ancón formations. could have contained a low abundance in planktonic foraminifera, explaining partly why reworked Cretaceous specimens are scarce and/or absent in both formations. The lowermost Danian planktonic foraminiferal assemblages of Moncada thus suggest that only *Guembelitria* species seem to have survived the K/Pg boundary mass extinction as originally suggested by Smit (1982).

The large amount of CO₂ gas devolatilized in the meteorite impact could have initiated an intense global warming by a greenhouse effect after the "impact winter" phase (see Kawaragi et al., 2009), persisting for thousands of years. In addition, the pollution of the oceans by contaminants of meteoritic origin could have persisted for at least 10 to 20kyr after the K/Pg boundary (a time interval equivalent to the G. cretacea zone), as suggested in Moncada and other sections worldwide. These stressed conditions in the surface pelagic environment may explain the peak in Guembelitria (PFAS-1) for approximately 10kyr after the K/Pg boundary (a time interval equivalent to the deposition of the "K/T Boundary Clay"), and the subsequent evolutionary radiation and acme of parvularugoglobigerinids (PFAS-2). Guembelitria comprises opportunist, r-strategy species that mainly inhabited nutrient-rich shallow, neritic waters (Kroon and Nederbragt, 1990; Olsson et al., 1999), so it may have been the only Cretaceous planktonic foraminifera taxon that could withstand the short- and long-term environmental stress conditions generated after the Chicxulub impact event, dominating the PFAS-1 for the first 10kyr after the K/Pg boundary. Parvularugoglobigerinids, which dominated the PFAS-2 from 10 to 50kyr after the K/Pg boundary, were also likely r-strategy opportunists, which rapidly colonized and speciated at all latitudes after the re-establishment of the pelagic environmental conditions in terms of temperature, nutrients, etc. (Li et al., 1995). The evolutionary radiation of planktonic foraminifera in the earliest Danian (Arenillas et al., 2000) was due to the progressive environmental recovery after the short-term "impact winter" phase and the subsequent repopulation of vacated niches during the long-term greenhouse phase (Molina, 2015). We suggest that the rate of evolution could have been increased by the effect of the long-term pollution of the oceans by contaminants of meteoritic origin, which could have caused the heightening of mutation rates for a time interval of more than 10kyr after the K/Pg boundary.

CONCLUSIONS

The Moncada section, western Cuba, contains a lithostratigraphic unit called the Moncada Fm., which is enriched in ejecta material, including high Ir concentrations toward and above its top. This formation disconformably overlies the Albian micritic limestones of the Pons Fm. and is conformably overlain by the lowermost Danian marly limestones of the Ancón Fm. The Moncada Fm. is composed of altered melt rock fragments (broken glass spherules, shocked quartz grains, melt rock fragments, etc.), indicating that it is the local CCU genetically related to the Chicxulub impact. This CCU is overlain by a 2-3cm thick unit of Ir-rich, dark-colored, calcareous claystone called the UMU at Moncada. High-resolution planktonic foraminiferal biostratigraphy allowed us to identify all the lowermost Danian planktonic foraminiferal zones at Moncada, including the *H. holmdelensis* subzone or zone P0 within the UMU. As in most continuous K/Pg sections worldwide (e.g., El Kef, Tunisia, and Bochil, Mexico), the lowermost Danian PFAS were also identified at Moncada, including the Guembelitria acme (PFAS 1) within the UMU and the basal part of the Ancón Fm. Petrographic and planktonic foraminiferal data therefore indicate that the ejecta-rich Moncada Fm. is K/Pg boundary in age, and that the UMU represents the "K/T Boundary Clay" at Moncada.

Except for *Guembelitria* species, the absence of cosmopolitan, generalist Cretaceous species in the lowermost Danian of Moncada suggests that the mass extinction of planktonic foraminifera at the K/Pg boundary was more severe and catastrophic than previously suggested. Only opportunist *Guembelitria* species seem to have survived the mass extinction triggered by the Chicxulub impact event. The global warming caused by an increased

greenhouse effect after the "impact winter" phase and, as suggested at Moncada and other sections worldwide, the pollution of the oceans by contaminants of meteoritic origin could have caused ecological stress conditions in the surface pelagic environment lasting at least 10 to 20kyr after the K/Pg boundary. These paleoenvironmental factors are sufficient to explain the initial acme of *Guembelitria* (PFAS-1) and the subsequent evolutionary radiation and acme of parvularugoglobigerinids (PFAS-2).

ACKNOWLEDGMENTS

We thank Paul Pearson and Matthew Powell for helpful comments. This research was funded by the Spanish Ministerio de Economía y Competitividad projects CGL2015-64422-P, CGL2011-23077 and CGL2011-22912 (cofinanced by European Regional Development Fund), UZ2015-CIE-02 (funded by the Universidad de Zaragoza, Spain), the Aragonian Departamento de Educación y Ciencia (DGA group E05) and the European Social Fund (ESF). Authors would also like to acknowledge the use of Servicio General de Apoyo a la Investigación-SAI, Universidad de Zaragoza.

REFERENCES

Aberhan, M., Weidemeyer, S., Kiessling, W., Scasso, R.A., Medina, F.A., 2007. Faunal evidence for reduced productivity and uncoordinated recovery in Southern Hemisphere Cretaceous/Paleogene boundary sections. Geology, 35, 227-230.

Alegret, L., Arenillas, I., Arz, J.A., Díaz, C., Grajales-Nishimura, J.M., Meléndez, A., Molina, E., Rojas, R., Soria, A.R., 2005. Cretaceous/Paleogene (K/Pg) boundary clastic complex at Loma Capiro, Central Cuba: evidence for a K/Pg impact origin. Geology, 33, 721-724.

Alegret, L., Thomas, E., Lohman, K.C., 2011. End-Cretaceous marine mass extinction not caused by productivity collapse. Proceedings of the National Academy of Sciences (PNAS), 109(3), 728-732.

Arenillas, I., Arz, J.A., Molina, E., Dupuis, C., 2000. An independent test of planktic foraminiferal turnover across the Cretaceous/Paleogene (K/P) boundary at El Kef, Tunisia: Catastrophic mass extinction and possible survivorship. Micropaleontology, 46(1), 31-49.

Arenillas, I., Arz, J.A., Molina, E., 2004. A new high-resolution planktic foraminiferal zonation and subzonation for the lower Danian. Lethaia, 37, 79-95.

Arenillas, I., Arz, J.A., Grajales-Nishimura, J.M., Murillo-Muñetón, G., Alvarez, W., Camargo-Zanoguera, A., Molina, E., Rosales-Domínguez, C., 2006. Chicxulub impact event is Cretaceous/Paleogene boundary in age: new micropaleontological evidence. Earth and Planetary Science Letters, 249, 241-257.

- Arenillas, I., Arz, J.A., Grajales-Nishimura, J.M., Rosales-Domínguez, M.C., González-Lara, J.C., Maurrasse, F.J-M.R., Rojas-Consuegra, R., Murillo-Muñetón, G., Velasquillo-Martínez, L.G., Camargo-Zanoguera, A., Menéndez-Peñate, L., 2011. Integrated stratigraphy of the Cretaceous-Tertiary transition in the Gulf of Mexico: key horizons for recognition of oil reservoirs. Gulf Coast Association of Geological Societies (GCAGS) 61 (Transactions), 33-44.
- Arz, J.A., Arenillas, I., Soria, A.R., Alegret, L., Grajales-Nishimura, J.M., Liesa, C.L., Meléndez, A. Molina, E., Rosales, M.C., 2001. Micropaleontology and sedimentology across the Cretaceous/Tertiary boundary at La Ceiba (Mexico): Impact-generated sediment gravity flows. Journal of South American Earth Sciences, 14, 505-519.
- Arz, J.A., Alegret, L., Arenillas, I., 2004. Foraminiferal biostratigraphy and paleoenvironmental reconstruction at Yaxcopoil-1 drill hole (Chicxulub crater, Yucatan Peninsula). Meteoritics & Planetary Science, 39, 1099-1111.
- Berggren, W.A., Pearson, P.N., 2005. A revised tropical to subtropical Paleogene planktonic foraminiferal zonation. Journal of Foraminiferal Research, 35, 279-298.
- Blakey, R., 2011. Cretaceous-Tertiary (65Ma) North American paleogeographic map. Colorado Plateau Geosystems, INC. Last accessed: January 16th, 2015; website: www.cpgeosystems.com/nam.html
- Bohor, B.F., 1996. A sediment gravity flow hypothesis for siliciclastic units at the K/T boundary, northeastern Mexico. In: Ryder, G., Fastovsky, D., Garner, S. (eds.). The Cretaceous-Tertiary Event and other catastrophes in Earth history. Geological Society of America, 307 (Special Paper), 183-195.
- Bralower, T.J., Iturralde-Vinent, M.A., 1997. Micropaleontological dating of the collision between the North American plate and the Greater Antilles Arc in western Cuba. Palaios, 12, 133-150.
- Bralower, T.J., Paul, C.K., Leckie, R.M., 1998. The Cretaceous-Tertiary boundary cocktail: Chicxulub impact triggers margin collapse and extensive sediment gravity flows. Geology, 26, 331-334.
- Caron, M., 1985. Cretaceous planktic foraminifera. In: Bolli, H.M., Saunders, J.B., Perch-Nielsen, K. (eds.). Plankton Stratigraphy. Cambridge, Cambridge University Press, 17-86.
- Chenet, A.L., Auidelleur, X., Fluteau, F., Courtillot, V.Y. Bajpai, S., 2007. 40K-40Ar dating of the main Deccan large igneous province: Further evidence of KTB age and short duration. Earth and Planetary Science Letters, 263, 1-15.
- Claeys, P., Kiessling, W., Alvarez, W., 2002. Distribution of Chicxulub ejecta at the Cretaceous-Tertiary boundary. In: Koeberl, C., MacLeod, K.G. (eds.). Catastrophic events and mass extinctions: Impacts and beyond. Boulder (Colorado), Geological Society of America, 356 (Special Paper), 55-68.
- Colodner, D.C., Boyle, E.A., Edmond, J.M., Thomson, J., 1992. Post-depositional mobility of platinum, iridium and rhenium in marine sediments, Nature, 358, 402-404.
- Denne, R.A., Scott, E.D., Eickhoff, D.P., Kaiser, J.S., Kaiser, J.S., Hill, R.J., Spaw, J.M., 2013. Massive Cretaceous/Paleogene

- deposit, deep-water Gulf of Mexico: New evidence for widespread Chicxulub-induced slope failure. Geology, 41, 983-986.
- Dupuis, C., Steurbaut, E., Molina, E., Rauscher, R., Tribovillard, N.P., Arenillas, I., Arz, J.A., Robaszynski, F., Caron, M., Robin, E., Rocchia, R., Lefèvre, I., 2001. The Cretaceous-Paleogene (K/P) boundary in the Aïn Settara section (Kalaat-Senan, Central Tunisia): lithological, micropaleontological and geochemical evidence. Bulletin de l'Institut Royal des Sciences Naturelles de Belgique, 71, 169-190.
- Erickson, D.J., Dickson, S.M. 1987. Global trace-element biogeochemistry at the K/T boundary oceanic and biotic response to a hypothetical meteorite impact. Geology, 15, 1014-1017.
- García, D.E., Torres, A.I., 1997. Sistema Paleógeno. In: Furrazola-Bermúdez, G., Núñez-Cambra, K.E. (eds.). Estudios de Geología de Cuba. La Habana, Centro Nacional de Información Geológica, Instituto de Geología y Paleontología, 115-164.
- Grajales-Nishimura, J.M., Cedillo-Pardo, E., Rosales-Domínguez, M.C., Morán-Zenteno, D.J., Alvarez, W., Claeys, P., Ruiz-Morales, J., García-Hernandez, J., Padilla-Avila, P., Sánchez-Ríos, A., 2000. Chicxulub impact: The origin of reservoir and seal facies in the southeastern Mexico oil fields. Geology, 28, 307-310.
- Grajales-Nishimura, J.M., Murillo-Muñetón, G., Rosales-Domínguez, M.C., Cedillo-Pardo, E., García-Hernández, J., 2003. Heterogeneity of lithoclast composition in the deepwater carbonate breccias of the K/T boundary sedimentary succession, southeastern Mexico and offshore Campeche. American Association of Petroleum Geologists, 79 (Memoir), 312-329.
- Grajales-Nishimura, J.M., Murillo-Muñetón, G., Rosales-Domínguez, M.C., Bermúdez-Santana, J.C., Velasquillo-Martínez, L.G., García-Hernández, J., Arz, J.A., I. Arenillas, I., 2009. The Cretaceous-Paleogene boundary Chicxulub Impact: Its effect on carbonate sedimentation on the western margin of the Yucatan Platform and nearby areas. In: Bartolini, C., Román-Ramos, J.R. (eds.). Petroleum systems in the southern Gulf of Mexico. American Association of Petroleum Geologists (AAPG), 90 (Memoir), 315-335.
- Goto, K., Tada, R., Tajika, E., Matsui, T., 2008. Deep-sea tsunami deposits in the Proto-Caribbean Sea at the Cretaceous/Tertiary boundary. In: Shiki, T., Tsuji, Y., Minoura, K., Yamazaki, T. (eds.). Tsunamiites - Features and Implications. Elsevier B.V., 251-275.
- Hildebrand, A.R., Penfield, G.T., Kring, D.A., Pilkington, M., Camargo, Z.A., Jacobsen, S.B., Boynton, W.V., 1991. Chicxulub crater: a possible Cretaceous/Tertiary boundary impact crater on the Yucatan Peninsula, Mexico. Geology, 19, 867-871.
- Huber, B.T., 1996. Evidence for planktonic foraminifer reworking versus survivorship across the Cretaceous-Tertiary boundary at high latitudes. In: Ryder, G., Fastovsky, D.E., Gartner, S. (eds.). The Cretaceous-Tertiary event and other catastrophes

- in Earth history. Geological Society of America, 307 (Special Paper), 319-334.
- Huber, B.T., Macleod, K.G., Norris, R.D., 2002. Abrupt extinction and subsequent reworking of Cretaceous planktonic foraminifera across the K/T boundary: evidence from the subtropical North Atlantic. In: Koeberl, C., MacLeod, K. (eds.). Catastrophic Events and Mass Extinctions: Impacts and Beyond. Geological Society of America, 356 (Special Paper), 227-289.
- Iturralde-Vinent, M., 1995. Sedimentary Geology of Western Cuba. Linked Earth Systems. In: Field Guide, 1st Congress on Sedimentary Geology. Society for Sedimentary Geology (SEPM), 1-21.
- Iturralde-Vinent, M., 1998. Sinopsis de la constitución geológica de Cuba. In: Melgarejo, J.C., Proenza, J.A. (eds.). Geología y metalogenia de Cuba: Una introducción. Acta Geológica Hispánica, 33(1-4), 9-56.
- Iturralde-Vinent, M. (ed.), 2012. Compendio de Geología de Cuba y el Caribe. Segunda Edición, DVD-ROM., CITMATEL, ISBN 9-789592-572863.
- Izett, G.A., Maurrasse, F.J.-M.R., Lichte, F.E., Meeker, G.P., Bates, R., 1990. Tektites in Cretaceous-Tertiary boundary rocks on Haiti. U.S. Geological Survey Open-File Report, 90, 1-31.
- Kaiho, K., Lamolda, M.A., 1999. Catastrophic extinction of planktonic foraminifera at the Cretaceous-Tertiary boundary evidenced by stable isotopes and foraminiferal abundance at Caravaca, Spain. Geology, 27(4), 355-358.
- Kawaragi, K., Sekine, Y., Kadono, T., Sugita, S., Ohno, S., Ishibashi, K., Kurosawa, K., Matsui, T., Ikeda, S., 2009. Direct measurements of chemical composition of shockinduced gases from calcite: an intense global warming after the Chicxulub impact due to the indirect greenhouse effect of carbon monoxide. Earth and Planetary Science Letters, 282(1-4), 56-64.
- Keller, G., Stinnesbeck, W., Adatte, T., Stueben, D., 2003. Multiple impacts across the Cretaceous-Tertiary boundary. Earth-Science Reviews, 62, 327-363.
- Keller, G., Adatte, T., Berner, Z., Harting, M., Baum, G., Prauss, M., Tantawy, A.-A., Stueben, D., 2007. Chicxulub Impact Predates K-T Boundary: New Evidence from Brazos, Texas. Earth and Planetary Science Letters, 255, 339-356.
- Kroon, D., Nederbragt, A.J., 1990. Ecology and paleoecology of triserial planktic foraminifera. Marine Micropaleontology, 16, 25-38.
- Lee, C.T., Wasserburg, G.J., Kyte, F.T., 2003. Platinum group elements (PGE) and rhenium in marine sediments across the Cretaceous–Tertiary boundary: constraints on Re-PGE transport in the marine environment. Geochimica et Cosmochimica Acta, 67, 655-670.
- Li, Q., McGowran, B., Boersma, A., 1995. Early Paleocene Parvularugoglobigerina and late Eocene Praetenuitella: does evolutionary convergence imply similar habitat? Journal of Micropaleontology, 14, 119-134.
- MacLeod, K.G., Whitney, D.L., Huber, B.T., Koeberl, C., 2007. Impact and extinction in remarkably complete Cretaceous—

- Tertiary boundary sections from Demerara Rise, tropical western North Atlantic. Geological Society of America Bulletin, 119, 101-15.
- Martínez-Ruiz, F., Ortega-Huertas, M., Palomo-Delgado, I.,
 Smit, J., 2001. K–T boundary spherules from Blake Nose (ODP Leg 171B) as a record of the Chicxulub ejecta deposits.
 In: Kroon, D., Norris, R.D., Klaus, A. (eds.). Western North Atlantic Paleogene and Cretaceous Paleoceanography.
 Geological Society of London, 183 (Special Publication), 183, 149-161.
- Maurrase, F.J.-M.R., Sen, G., 1991. Impacts, tsunamis, and the Haitian Cretaceous-Tertiary boundary layer. Science, 252, 1690-1693.
- Maurrasse, F.J.-M.R., Lamolda, M.A., Aguado, R., Peryt, D., Sen, G., 2005. Spatial and temporal variations of the Haitian K/T Boundary record: implications concerning the event or events. Journal of Iberian Geology, 31, 113-133.
- Molina, E., 2015. Evidence and causes of the main extinction events in the Paleogene based on extinction and survival patterns of foraminifera. Earth-Science Reviews, 140, 166-181.
- Molina, E., Alegret, L., Arenillas, I., Arz, J.A., Gallala, N., Hardenbol, J., von Salis, K., Steurbaut, E., Vandenberghe, N., Zaghbib-Turki, D., 2006. The Global Stratotype Section and Point of the Danian Stage (Paleocene, Paleogene, "Tertiary", Cenozoic) at El Kef, Tunisia: original definition and revision. Episodes, 29(4), 263-278.
- Molina, E., Alegret, L., Arenillas, I., Arz, J.A., Gallala, N., Grajales-Nishimura, M., Murillo-Muñetón, G., Zaghbib-Turki, D., 2009. The Global Boundary Stratotype Section and Point for the base of the Danian Stage (Paleocene, Paleogene, "Tertiary", Cenozoic): auxiliary sections and correlation. Episodes, 32(2), 84-95.
- Montanari, A., Claeys, P., Asaro, F., Bermúdez, J., Smit, J., 1994.
 Preliminary stratigraphy and Iridium and other geochemical anomalies across the K/T boundary in the Bochil section (Chiapas, southeastern Mexico). Lunar and Planetary Institute Contributions, 825, 84-85.
- Morgan, J.V., Lana, C., Kearsley, A., Coles, B., Belcher, C., Montanari, S., Díaz-Martínez, E., Barbosa, A., Neumann, V., 2006. Analyses of shocked quartz at the global K–P boundary indicate an origin from a single, high-angle, oblique impact at Chicxulub. Earth and Planetary Science Letters, 251(3-4), 264-279.
- Norris, R.D., Huber, B.T., Self-Trail, J., 1999. Synchroneity of the KT oceanic mass extinction and meteorite impact: Blake Nose, western North Atlantic. Geology, 27, 419-422.
- Olsson, R.K., Miller, K.G., Browning, J.V., Habib, D., Sugarmann, P.J., 1997. Ejecta layer at the Cretaceous-Tertiary boundary, Bass River, New Jersey (Ocean Drilling Program Leg 174AX). Geology, 25, 759-762.
- Olsson, R.K., Hemleben, C., Berggren, W.A., Huber, B.T., 1999. Atlas of Paleocene Planktonic Foraminifera. Smithsonian Contributions to Paleobiology, 85, 1-252.
- Petrizzo, M.R., 2002. Palaeoceanographic and palaeoclimatic inferences from Late Cretaceous planktonic foraminiferal

- assemblages from the Exmouth Plateau (ODP Sites 762 and 73, eastern Indian Ocean). Marine Micropaleontology, 45(2), 117-150.
- Premovic, P.I., Todorovic, B.Z., Stankovic, M.N., 2008. Cretaceous-Paleogene boundary (KPB) Fish Clay at Højerup (Stevns Klint, Denmark): Ni, Co, and Zn of the black marl. Geologica Acta, 6(4), 369-382.
- Pszczólkowski, A., 1987. Secuencias miogeosinclinales de la Cordillera de Guaniguanico; su litoestratigrafía, desarrollo de facies, paleogeografía. In: Pszczólkowski, A., Piotrowska, K., Piotrowski, J., Torre De La, A., Myczynski, R., Haczewski, G. (eds.). Contribución a la geología de la provincia de Pinar del Río. La Habana, Científico-Técnica, Academia de Ciencias de Cuba. 5-84.
- Renne, P.R., Deino, A.L., Hilgen, F.J., Kuiper, K.F., Mark, D.F., Mitchell, W.S, Morgan, L.E., Mundil, R., Smit, J., 2013. Time scales of critical events around the Cretaceous–Paleogene boundary. Science, 339, 684-687.
- Rodríguez-Tovar, F.J., Uchman, A., Molina, E., Monechi, S., 2010. Bioturbational redistribution of Danian calcareous nannofossils in the uppermost Maastrichtian across the K-Pg boundary at Bidart, SW France. Geobios, 43, 569-579.
- Schoene, B., Samperton, K.M., Eddy, M.P., Keller, G., Adatte, T., Bowring, S.A., Khadri, S.F.R., Gerch, B., 2015. U-Pb geochronology of the Deccan Traps and relation to the end-Cretaceous mass extinction. Science 347(6218), 182-184.
- Schulte, P., Alegret, L., Arenillas, I., Arz, J.A., Barton, P.J., Bown, P.R., Bralower, T.J., Christeson, G.L., Claeys, P., Cockell, C.S., Collins, G.S., Deutsch, A., Goldin, T.J., Goto, K., Grajales-Nishimura, J.M., Grieve, R.A.F., Gulick, S.P.S., Johnson, K.R., Kiessling, W., Koeberl, C., Kring, D.A., MacLeod, K.G., Matsui, T., Melosh, J., Montanari, A., Morgan, J.V., Neal, C.R., Norris, R.D., Pierazzo, E., Ravizza, G., Rebolledo-Vieyra, M., Reimold, W.U., Robin, E., Salge, T., Speijer, R.P., Sweet, A.R., Urrutia-Fucugauchi, J., Vajda, V., Whalen, M.T., Willumsen, P.S., 2010. The Chicxulub asteroid impact and mass extinction at the Cretaceous-Paleogene boundary. Science, 327(5970), 1214-1218.
- Scott, E., Denne, R., Kaiser, J., David Eickhoff, D., 2014. Impact on Sedimentation into the North-Central Deepwater Gulf of Mexico as a Result of the Chicxulub Event. Gulf Coast Association of Geological Societies (GCAGS) Journal, 3, 41-50.
- Sigurdsson, H., D'Hondt, S., Arthur, M.A., Bralower, T.J., Zachos, J.C., Fossen, M.V., Channell, E.T., 1991. Glass from the Cretaceous/Tertiary boundary in Haiti. Nature, 349(6309), 482-487.
- Smit, J., 1982. Extinction and evolution of planktonic foraminifera after a major impact at the Cretaceous/Tertiay boundary. Geological Society of America, 190 (Special Paper), 329-352.

- Smit, J., 1999. The global stratigraphy of the Cretaceous-Tertiary Boundary impact ejecta. Annual Review of Earth and Planetary Science, 27, 75-113.
- Smit, J., Romein, A.J.T., 1985. A sequence of events across the Cretaceous-Tertiary boundary. Earth and Planetary Science Letters, 74, 155-170.
- Smit, J., Montanari, A., Swiburne, N.H.M., Alvarez, W., Hildebrand, A.R., Margolis, S.V., Claeys, P., Lowrie, W., Asaro, F., 1992. Tektite-bearing, deep-water Clastic Unit at the Cretaceous-Tertiary boundary in northeastern Mexico. Geology, 20, 99-103.
- Smit, J., Roep, T.B., Alvarez, W., Montanari, A., Claeys, P., Grajales-Nishimura, J.M., Bermudez, J., 1996. Coarsegrained, clastic sandstone complex at the K/T boundary around the Gulf of Mexico: Deposition by tsunami waves induced by the Chicxulub impact? Geological Society of America, 307 (Special Paper), 151-182.
- Soria, A.R., Liesa, C., Mata, P., Arz, J.A., Alegret, L., Arenillas, I., Meléndez, A., 2001. Slumping and a sandbar deposit at the K/T boundary in the El Tecolote sector (northeastern Mexico): An impact-induced sediment gravity flow. Geology, 29, 231-234.
- Tada, R., Nakano, Y., Iturralde-Vinent, M.A., Yamamoto, S.,
 Kamata, T., Tajika, E., Toyoda, K., Kiyokawa, S., Delgado,
 D.G., Oji, T., Goto, K., Takayama, H., Rojas-Consuegra,
 R., Matsui, T., 2002. Complex tsunami waves suggested by
 the Cretaceous/Tertiary boundary deposit at the Moncada
 section, western Cuba. In: Koeberl, C., Macleod, G. (eds.).
 Catastrophic Events and Mass Extinctions: Impact and
 Beyond. Geological Society of America, 356 (Special Paper),
 109-123
- Tada, R., Iturralde-Vinent, M.A., Matsui, T., Tajika, E., Oji, T., Goto, K., Nakano, Y., Takayama, H., Yamamoto, S., Rojas-Consuegra, R., Kiyokawa, S., García-Delgado, D.E., Díaz-Otero, C., Toyoda, K., 2003. K/T boundary deposits in the proto-Caribbean basin. American Association of Petroleum Geologists (AAPG), 79 (Memoir), 582-604.
- Tagle, R., Claeys, P., 2001. Platinum group element (PGE) distribution in ejecta and impactites from Chicxulub. Granada, Spain, 6th ESF-IMPACT Workshop "Impact Marker in the Stratigraphic Record", Abstract Book, 129.
- Takayama, H., Tada, R., Matsui, T., Iturralde-Vinent, M.A., Oji, T., Tajika, E., Kiyokawa, S., García, D.G., Okada, H., Hasegawa, T., Toyoda, K., 2000. Origin of the Peñalver Formation in northwestern Cuba and its relation to K/T boundary impact event. Sedimentary Geology, 135, 295-320.
- Vellekoop, J., Sluijs, A., Smit, J., Schouten, S., Weijers, J.W.H., Damsté, J.S.S., Brinkhuis, H., 2014. Rapid short-term cooling following the Chicxulub impact at the Cretaceous-Paleogene boundary. Proceedings of the National Academy of Sciences (PNAS), 111(21), 7537-7541.

Manuscript received March 2015; revision accepted October 2015; published Online January 2016.